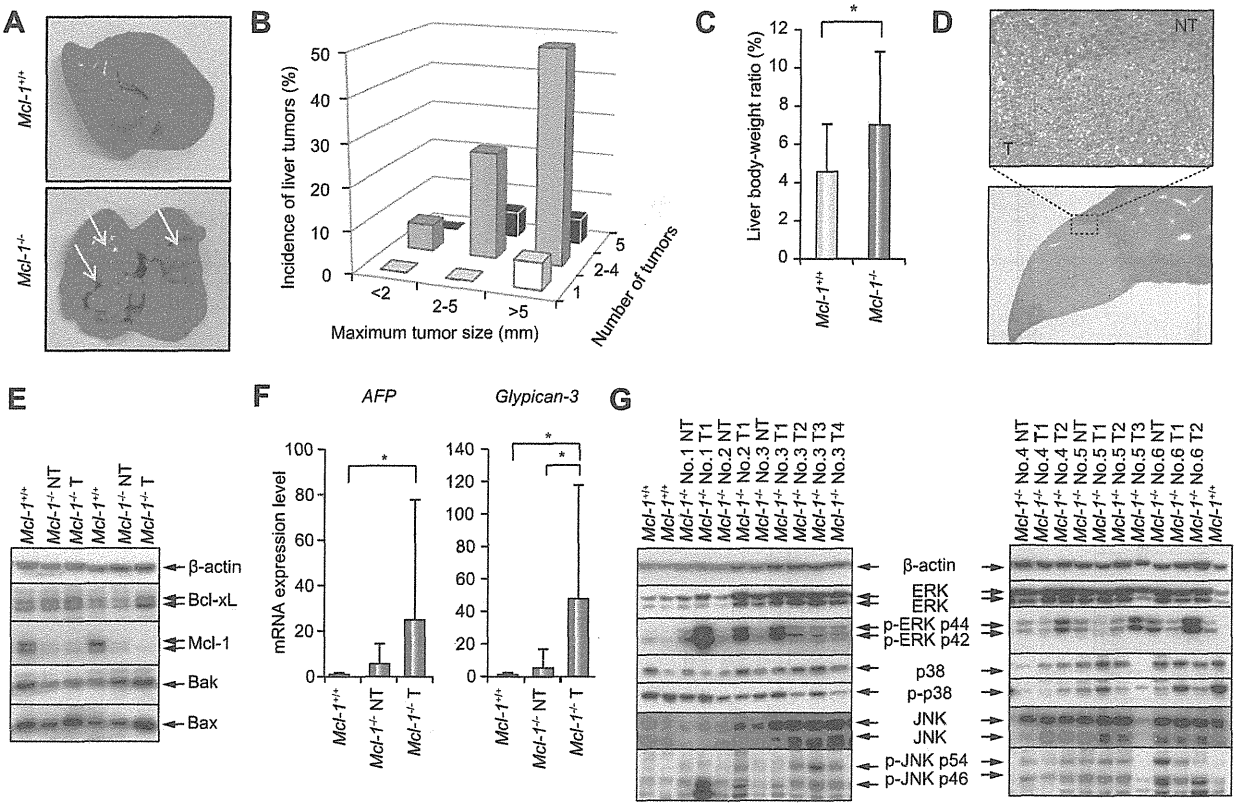

Fig. 2. Liver tumors in *Mcl-1* KO mice. (A–E) Hepatocyte-specific *Mcl-1*-deficient mice (*Mcl-1*$^{-/-}$) (N = 16) and their control littermates (*Mcl-1*$^{+/+}$) (N = 22) were sacrificed at 1.5 years of age. (A) Representative macroscopic view of the livers with arrows indicating tumors. (B) Incidence of liver tumors separated by maximum tumor size and number of tumors. (C) Liver body-weight ratio. (D) Representative histology of liver tumors in *Mcl-1* KO mice. (E) Western blot of the Bcl-2 family proteins in tumors (T) and surrounding non-cancerous livers (NT) of *Mcl-1* KO mice and livers of control mice. (F and G) Characteristics of liver tumors in *Mcl-1* KO mice. (F) Real-time RT-PCR analysis of the expression levels of α-fetoprotein (*AFP*) and *glypican*-3 mRNA (N = 16 per group). (G) Expression and activation of mitogen-activated protein kinases. *p <0.05.

KO mice as evidenced by TUNEL staining of liver sections, serum ALT levels and caspase-3/7 activity at 6 weeks of age (Fig. 4A–C). Weber *et al.* [12] previously described hepatocyte regeneration in the *Mcl-1* KO liver. In agreement with this, *Mcl-1* KO livers showed higher expression of cell cycle markers PCNA and ki-67, than those from control littermates (Fig. 4A, B, and D and Supplementary Fig. 4). Importantly, the levels of PCNA and ki-67 expression decreased with a *Bak* KO background in *Mcl-1* KO mice. While *Mcl-1* KO livers show a mild fibrotic change [11], the levels of col1a1 expression at 6 weeks of age and Sirius red staining at 1 year of age decreased with a *Bak* KO background in *Mcl-1* KO livers (Fig. 4E and Supplementary Fig. 5). Bak deficiency also reduced expression levels of TNF-α, MCP-1, and CD68 at 6 weeks of age (Fig. 4F). Next, we examined the impact of apoptosis inhibition by Bak deficiency on oxidative stress markers, which were increased in *Mcl-1* KO livers. Real-time RT-PCR revealed that Bak deficiency reduced the levels of HO-1 and NQO1 expression at 6 weeks of age (Fig. 4G). Consistent with these observations, *Bak* KO significantly lowered the number of 8-OHdG-positive nuclei in *Mcl-1* KO livers at 1 year of age (Fig. 4H). These results suggested that inhibition of hepatocyte apoptosis reduced oxidative stress in the liver. Finally, to examine the impact of apoptosis inhibition on liver tumor development, we compared the carcinogenetic rates in *Mcl-1* KO mice with or without *Bak* KO background at 1 year of age and found that *Bak* KO significantly suppressed liver tumor development (Fig. 5A and B and Table 1).

Discussion

Mcl-1 was first identified as a gene induced during myeloid cell differentiation. Compared with other anti-apoptotic members such as Bcl-2, Bcl-xL, Bcl-w, and Bfl-1, Mcl-1 possesses a unique N-terminus containing two PEST domains, which are found in proteins displaying rapid turnover, and its expression is tightly regulated by growth factors and a variety of other stimuli. Mice systemically deficient for Bcl-xL suffered embryonic death due to massive apoptosis in hematopoietic organs and developing neurons [22]. On the other hand, systemic *Mcl-1* KO resulted in peri-implantation lethality, but *Mcl-1* KO embryos showed no alterations in the extent of apoptosis [23], suggesting that Mcl-1 may play a role early in development that is distinct from its anti-apoptotic functions. Indeed, *in vitro* studies have shown that Mcl-1 interacts with PCNA and Cdk1 in the nucleus and inhibits proliferation [13,14]. Recently, the early responding gene *IEX-1*

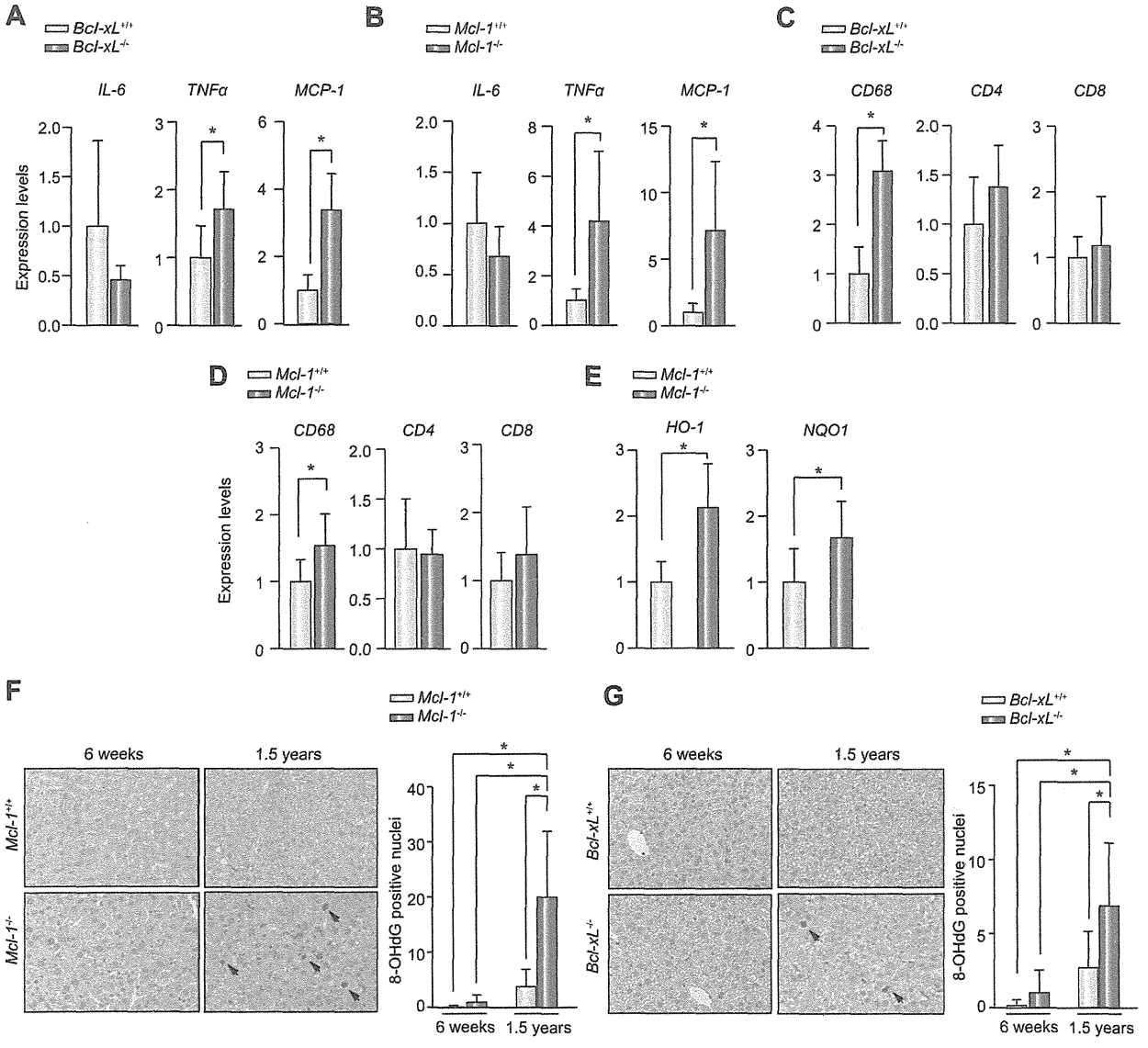

Fig. 3. Inflammatory response and oxidative stress in *Bcl-xL* or *Mcl-1* KO liver. (A–D) Inflammatory responses in KO livers. (A and C) Hepatocyte-specific *Bcl-xL* KO mice (*Bcl-xL*$^{-/-}$) and their control littermates (*Bcl-xL*$^{+/+}$) (N = 6 per group) as well as (B and D) hepatocyte-specific *Mcl-1* KO (*Mcl-1*$^{-/-}$) mice and their control littermates (*Mcl-1*$^{+/+}$) (N = 9 per group) were sacrificed at 6 weeks of age. Expression levels of (A and B) inflammatory molecules and (C and D) cell surface markers of immune cells were analyzed by real-time RT-PCR. (E–G) Oxidative injury in KO livers. (E) Real-time RT-PCR analysis of the expression levels of *HO-1* and *NQO1* of *Mcl-1* KO and control livers at 6 weeks of age (N = 9 per group). (F) Liver sections of *Mcl-1* KO or (G) *Bcl-xL* KO and the control liver at the indicated ages stained with anti-8-OHdG and statistics of the number of positive nuclei (N = 6 and more per group) (G). *$p < 0.05$.

was found to be induced upon DNA damage and to be bound to and to transport Mcl-1 from the cytosol to the nucleus [15]. Mcl-1 was also reported to be induced upon DNA damage and to regulate the DNA damage response through activation of Chk1 [16]. These findings suggest that Mcl-1 possesses additional functions in cell cycle progression and the DNA damage response pathway. This raised concern as to whether the hepatocarcinogenesis observed in *Mcl-1* KO mice was actually related to increased apoptosis in the liver.

In the present study, we demonstrated that hepatocyte-specific destruction of Bcl-xL led to the development of liver cancer similarly to that in hepatocyte-specific *Mcl-1* KO mice. Although we could not completely exclude the possibility that Bcl-xL may have additional effects other than apoptosis, this finding clearly shows that hepatocarcinogenesis observed in the apoptosis-prone liver is not a specific finding of loss of Mcl-1 but is also observed with the knockout of other genes that are critically involved in hepatocyte integrity. Tumors observed in these murine livers frequently showed activation of ERK and JNK, similar to the activation observed in human HCC [18,19]. While 64% of *Mcl-1* KO mice (14/22) developed liver tumors within 1 year, only 27% of *Bcl-xL* KO mice (3/11) did so within 1 year (Table 1). These finding indicate that the incidence rate of carcinogenesis in *Bcl-xL* KO mice is lower than that of *Mcl-1* KO mice. This may be

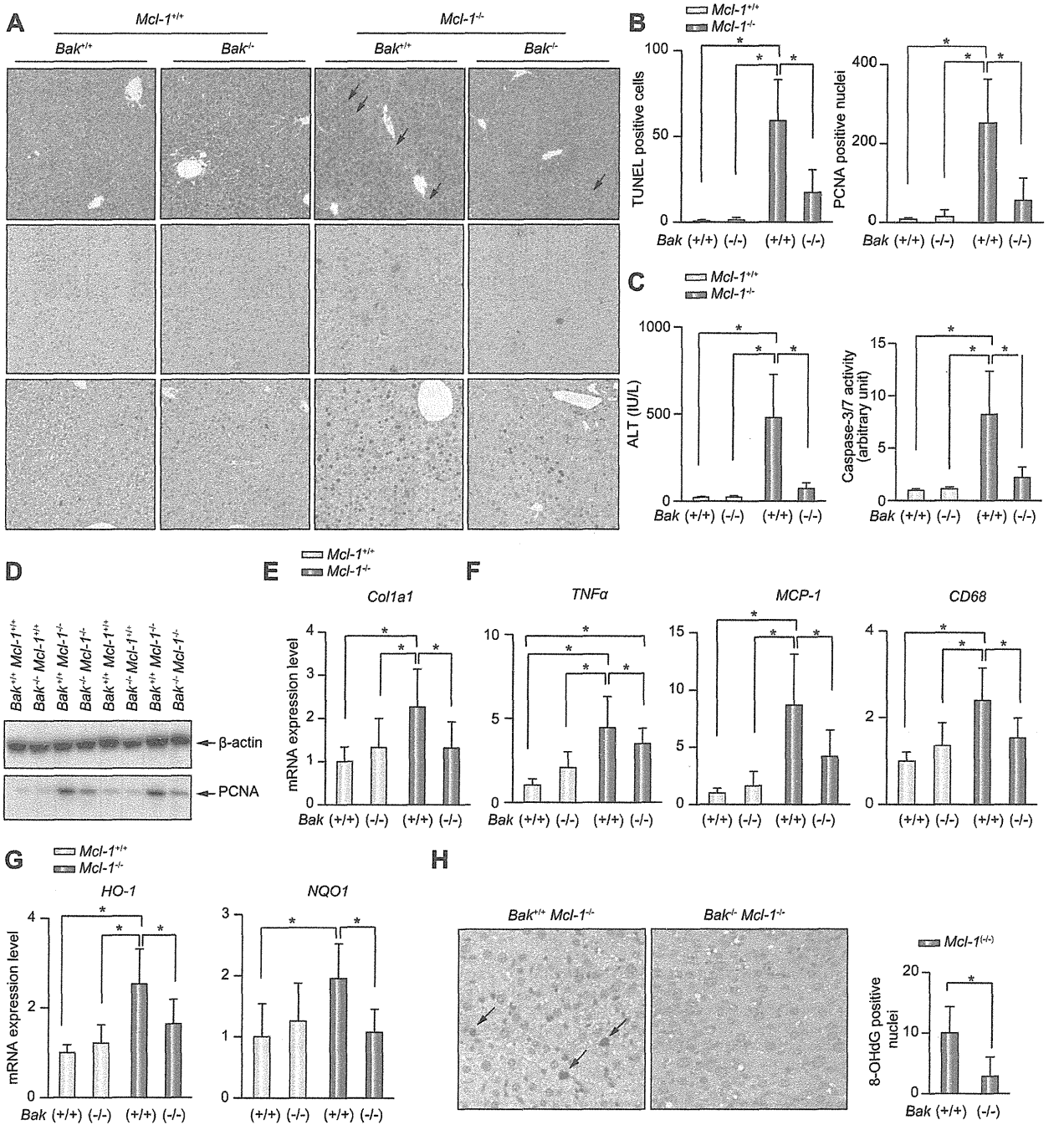

Fig. 4. Impact of Bak deficiency in *Mcl-1* KO mice. (A–G) *Bak*-deficient hepatocyte-specific *Mcl-1* KO mice ($Bak^{-/-}$ $Mcl\text{-}1^{-/-}$) were sacrificed at 6 weeks of age. (A) Representative pictures of hematoxylin–eosin with arrows indicating typical apoptotic cells (upper), TUNEL (middle) and PCNA staining (lower) and (B) statistics of TUNEL and PCNA staining of liver sections (N = 6 or 8 per group). (C) Serum levels of ALT and caspase-3/7 activity (N = 12 per group). (D) Western blot for PCNA expression. Real-time RT-PCR analysis for expression levels of (E) *Col1a1*, (F) *TNF-α*, *MCP-1*, *CD68*, (G) *HO-1* and *NQO1* in the livers at 6 weeks of age (N = 12 per group). (H) Liver sections of the *Bak*-deficient *Mcl-1* KO and control *Mcl-1* KO liver at 1 year of age stained with anti-8-OHdG. Representative images of liver sections stained with anti-8-OHdG (left) and statistics of the number of positive nuclei (N = 9 or 7 per group) (right). *p <0.05.

explained by the difference in levels of hepatocyte apoptosis and serum ALT, which are higher in *Mcl-1* KO mice than in *Bcl-xL* KO mice of the same age [10,11].

Mcl-1 executes its anti-apoptotic function by either directly or indirectly inhibiting the pro-apoptotic functions of Bak and/or Bax [24]. In the present study, we have shown that deletion of the *bak*

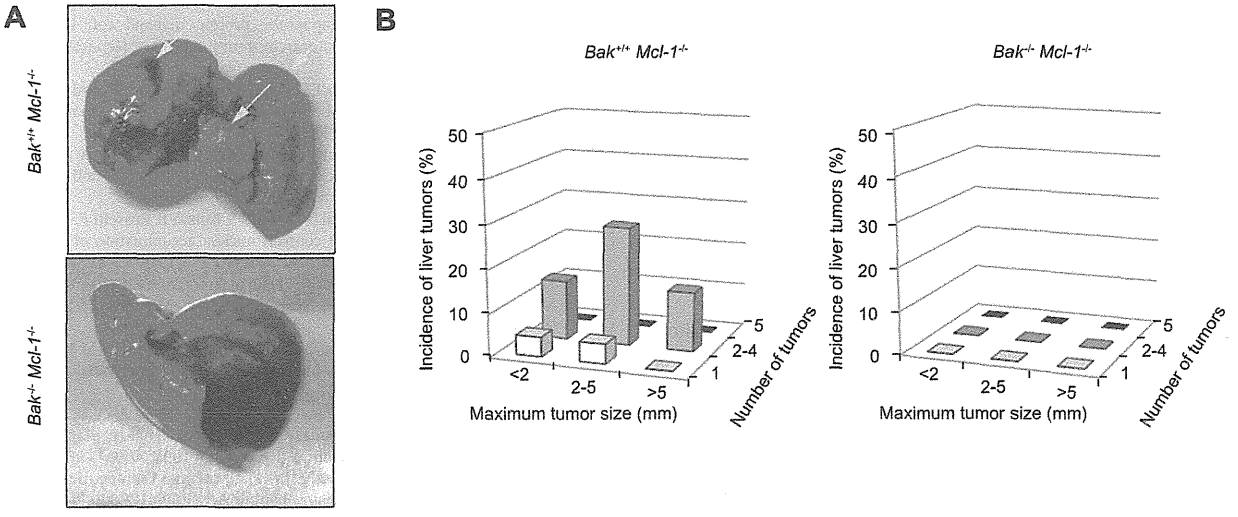

Fig. 5. Liver of aged *Bak/Mcl-1* double KO mice. (A and B) *Bak*-deficient *Mcl-1* KO mice ($Bak^{-/-}$ $Mcl\text{-}1^{-/-}$) (N = 7) and control *Mcl-1* KO mice ($Bak^{+/+}$ $Mcl\text{-}1^{-/-}$) (N = 22) were sacrificed at 1 year of age. (A) Representative macroscopic view of the livers with arrows indicating tumors. (B) Incidence of liver tumors separated by maximum tumor size and number of tumors.

gene resulted in a clear reduction in hepatocyte apoptosis in *Mcl-1* KO mice. Of importance is the finding that *bak* deletion leads to reduction of the liver regenerative response in *Mcl-1* KO mice. Bak is exclusively localized at the mitochondria in hepatocytes [25] and, upon exposure to apoptotic stimuli, undergoes oligomerization to form pores in the outer membrane of mitochondria, releasing cytochrome c, which in turn activates caspases. Since Bak is not involved in the activity of Mcl-1 in the nucleus, our present finding suggests that the regeneration observed in the *Mcl-1* KO liver is not due to loss of the Mcl-1 anti-proliferative effect but mainly to the compensatory regeneration of increased apoptosis. Most importantly, *bak* deletion clearly leads to reduced liver tumor incidence. This finding strongly suggests that the hepatocarcinogenesis observed in *Mcl-1* KO mice can be mostly ascribed to increased apoptosis in hepatocytes.

What does make hepatocytes undergo malignant transformation in the liver with increasing apoptosis? Regeneration is a physiological process in the liver like that in bone marrow or the intestine and compensatory liver regeneration itself is probably not sufficient to induce liver cancer [26]. The present study raised the possibility that TNF-α and oxidative stress are candidate factors responsible for the malignant transformation in the apoptosis-prone liver. TNF-α is reported to be a potent endogenous mutagen that promotes cellular transformation [20], and oxidative stress is reported to cause DNA damage leading to carcinogenesis [21]. Our results revealed that both TNF-α and oxidative stress were significantly increased in KO livers, and importantly, that inhibition of apoptosis by deletion of the *bak* gene reduced the levels of TNF-α and oxidative stress with a decrease in the tumorigenic rate. Some studies have shown that TNF-α induces oxidative stress in hepatocytes [27,28], while oxidative stress promotes production of inflammatory cytokines [29–31]. Taken together, oxidative stress and inflammatory cytokines may positively affect each other to turn healthy hepatocytes into malignant transformed hepatocytes in the liver of KO mice. Further studies are needed to examine the role of oxidative stress and inflammatory cytokines in apoptosis-induced hepatocarcinogenesis.

Apoptosis resistance has been established as a hallmark of cancer [32]. Indeed, accumulating evidence indicates that human HCC frequently overexpresses a variety of molecules which confer apoptosis resistance, such as anti-apoptotic Bcl-2 family proteins, Bcl-xL [33] and Mcl-1 [34,35]. Their overexpression was found to be associated with malignant phenotypes of tumors and poor prognosis of patients [36]. In the present study, tumors that developed in *Bcl-xL* or *Mcl-1* KO mice lacked expression of the respective proteins but reciprocally overexpressed Mcl-1 or Bcl-xL at high rates. We recently reported that conditional expression of Bcl-xL in tumor cells was translated into higher tumor growth in xenograft models [37], indicating that overexpression of anti-apoptotic Bcl-2 family proteins is important for tumor progression. Lack of Bcl-xL or Mcl-1 in hepatocytes generates persistent hepatocyte apoptosis leading to liver tumor development. On the other hand, reciprocal overexpression of Mcl-1 or Bcl-xL in the tumor of *Bcl-xL* or *Mcl-1* KO mice might be required for tumor progression.

Increasing evidence indicates that the serum level of ALT, a marker of hepatocyte apoptosis, is a risk factor for HCC in viral hepatitis [38] and non-alcoholic steatohepatitis [39]. A population-based study also revealed that elevated ALT levels raise the risk of liver cancer [40]. The present study provides evidence that spontaneous apoptosis in hepatocytes leads to liver cancer development and also offers genetic evidence that inhibition of apoptosis can help prevent liver cancer. Administration of caspase inhibitor was previously reported to lower serum ALT levels in patients with chronic hepatitis C [41]. It may be interesting and important, from a clinical point of view, to further determine whether pharmacological inhibition of apoptosis can be useful in preventing liver cancer development in *Bcl-xL* or *Mcl-1* KO mice.

Financial support

This work was partly supported by a Grant-in-Aid for Scientific Research from the Ministry of Education, Culture, Sports, Science, and Technology, Japan (to T. Tak.) and a Grant-in-Aid for Research

on Hepatitis from the Ministry of Health, Labour, and Welfare of Japan.

Conflict of interest

The authors who have taken part in this study declared that they do not have anything to disclose regarding funding or conflict of interest with respect to this manuscript.

Acknowledgements

We sincerely thank Dr. You-Wen He (Department of Immunology, Duke University Medical Center, Durham, NC) for providing the *mcl-1* floxed mice and Dr. Lothar Hennighausen (Laboratory of Genetics and Physiology, National Institute of Diabetes and Digestive and Kidney Diseases, National Institute of Health, Bethesda, MD) for providing the *Bcl-x* floxed mice.
This work was partly supported by a Grant-in-Aid for Scientific Research from the Ministry of Education, Culture, Sports, Science, and Technology, Japan (to T. Tak.) and Grant-in-Aid for Research on Hepatitis from the Ministry of Health, Labour and Welfare of Japan.

Supplementary data

Supplementary data associated with this article can be found, in the online version, at http://dx.doi.org/10.1016/j.jhep.2012.01.027.

References

[1] Malhi H, Gores G. Cellular and molecular mechanisms of liver injury. Gastroenterology 2008;134:1641–1654.
[2] Hiramatsu N, Hayashi N, Katayama K, Mochizuki K, Kawanishi Y, Kasahara A, et al. Immunohistochemical detection of Fas antigen in liver tissue of patients with chronic hepatitis C. Hepatology 1994;19:1354–1359.
[3] Mochizuki K, Hayashi N, Hiramatsu N, Katayama K, Kawanishi Y, Kasahara A, et al. Fas antigen expression in liver tissues of patients with chronic hepatitis B. J Hepatol 1996;24:1–7.
[4] Feldstein A, Canbay A, Angulo P, Taniai M, Burgart L, Lindor K, et al. Hepatocyte apoptosis and fas expression are prominent features of human nonalcoholic steatohepatitis. Gastroenterology 2003;125:437–443.
[5] Kronenberger B, Wagner M, Herrmann E, Mihm U, Piiper A, Sarrazin C, et al. Apoptotic cytokeratin 18 neoepitopes in serum of patients with chronic hepatitis C. J Viral Hepat 2005;12:307–314.
[6] Papatheodoridis GV, Hadziyannis E, Tsochatzis E, Chrysanthos N, Georgiou A, Kafiri G, et al. Serum apoptotic caspase activity as a marker of severity in HBeAg-negative chronic hepatitis B virus infection. Gut 2008;57:500–506.
[7] Wieckowska A, Zein NN, Yerian LM, Lopez AR, McCullough AJ, Feldstein AE. In vivo assessment of liver cell apoptosis as a novel biomarker of disease severity in nonalcoholic fatty liver disease. Hepatology 2006;44:27–33.
[8] Moriya K, Fujie H, Shintani Y, Yotsuyanagi H, Tsutsumi T, Ishibashi K, et al. The core protein of hepatitis C virus induces hepatocellular carcinoma in transgenic mice. Nat Med 1998;4:1065–1067.
[9] Pikarsky E, Porat RM, Stein I, Abramovitch R, Amit S, Kasem S, et al. NF-kappaB functions as a tumour promoter in inflammation-associated cancer. Nature 2004;431:461–466.
[10] Takehara T, Tatsumi T, Suzuki T, Rucker Er, Hennighausen L, Jinushi M, et al. Hepatocyte-specific disruption of Bcl-xL leads to continuous hepatocyte apoptosis and liver fibrotic responses. Gastroenterology 2004;127:1189–1197.
[11] Hikita H, Takehara T, Shimizu S, Kodama T, Li W, Miyagi T, et al. Mcl-1 and Bcl-xL cooperatively maintain integrity of hepatocytes in developing and adult murine liver. Hepatology 2009;50:1217–1226.
[12] Weber A, Boger R, Vick B, Urbanik T, Haybaeck J, Zoller S, et al. Hepatocyte-specific deletion of the antiapoptotic protein myeloid cell leukemia-1 triggers proliferation and hepatocarcinogenesis in mice. Hepatology 2010;51:1226–1236.
[13] Fujise K, Zhang D, Liu J, Yeh ET. Regulation of apoptosis and cell cycle progression by MCL1. Differential role of proliferating cell nuclear antigen. J Biol Chem 2000;275:39458–39465.
[14] Jamil S, Sobouti R, Hojabrpour P, Raj M, Kast J, Duronio V. A proteolytic fragment of Mcl-1 exhibits nuclear localization and regulates cell growth by interaction with Cdk1. Biochem J 2005;387:659–667.
[15] Pawlikowska P, Leray I, de Laval B, Guihard S, Kumar R, Rosselli F, et al. ATM-dependent expression of IEX-1 controls nuclear accumulation of Mcl-1 and the DNA damage response. Cell Death Differ 2010;17:1739–1750.
[16] Jamil S, Mojtabavi S, Hojabrpour P, Cheah S, Duronio V. An essential role for MCL-1 in ATR-mediated CHK1 phosphorylation. Mol Biol Cell 2008;19:3212–3220.
[17] Takehara T, Hayashi N, Tatsumi T, Kanto T, Mita E, Sasaki Y, et al. Interleukin 1beta protects mice from Fas-mediated hepatocyte apoptosis and death. Gastroenterology 1999;117:661–668.
[18] Ito Y, Sasaki Y, Horimoto M, Wada S, Tanaka Y, Kasahara A, et al. Activation of mitogen-activated protein kinases/extracellular signal-regulated kinases in human hepatocellular carcinoma. Hepatology 1998;27:951–958.
[19] Chen F, Beezhold K, Castranova V. JNK1, a potential therapeutic target for hepatocellular carcinoma. Biochim Biophys Acta 2009;1796:242–251.
[20] Yan B, Wang H, Rabbani ZN, Zhao Y, Li W, Yuan Y, et al. Tumor necrosis factor-alpha is a potent endogenous mutagen that promotes cellular transformation. Cancer Res 2006;66:11565–11570.
[21] Lonkar P, Dedon PC. Reactive species and DNA damage in chronic inflammation: reconciling chemical mechanisms and biological fates. Int J Cancer 2011;128:1999–2009.
[22] Motoyama N, Wang F, Roth KA, Sawa H, Nakayama K, Negishi I, et al. Massive cell death of immature hematopoietic cells and neurons in Bcl-x-deficient mice. Science 1995;267:1506–1510.
[23] Rinkenberger JL, Horning S, Klocke B, Roth K, Korsmeyer SJ. Mcl-1 deficiency results in peri-implantation embryonic lethality. Genes Dev 2000;14:23–27.
[24] Willis SN, Chen L, Dewson G, Wei A, Naik E, Fletcher JI, et al. Proapoptotic Bak is sequestered by Mcl-1 and Bcl-xL, but not Bcl-2, until displaced by BH3-only proteins. Genes Dev 2005;19:1294–1305.
[25] Hikita H, Takehara T, Kodama T, Shimizu S, Hosui A, Miyagi T, et al. BH3-only protein bid participates in the Bcl-2 network in healthy liver cells. Hepatology 2009;50:1972–1980.
[26] Aravalli RN, Steer CJ, Cressman EN. Molecular mechanisms of hepatocellular carcinoma. Hepatology 2008;48:2047–2063.
[27] Kamata H, Honda S, Maeda S, Chang L, Hirata H, Karin M. Reactive oxygen species promote TNFalpha-induced death and sustained JNK activation by inhibiting MAP kinase phosphatases. Cell 2005;120:649–661.
[28] Schwabe RF, Brenner DA. Mechanisms of Liver Injury. I. TNF-alpha-induced liver injury: role of IKK, JNK, and ROS pathways. Am J Physiol Gastrointest Liver Physiol 2006;290:G583–G589.
[29] Bulua AC, Simon A, Maddipati R, Pelletier M, Park H, Kim KY, et al. Mitochondrial reactive oxygen species promote production of proinflammatory cytokines and are elevated in TNFR1-associated periodic syndrome (TRAPS). J Exp Med 2011;208:519–533.
[30] Nakahira K, Haspel JA, Rathinam VA, Lee SJ, Dolinay T, Lam HC, et al. Autophagy proteins regulate innate immune responses by inhibiting the release of mitochondrial DNA mediated by the NALP3 inflammasome. Nat Immunol 2011;12:222–230.
[31] Zhou R, Yazdi AS, Menu P, Tschopp J. A role for mitochondria in NLRP3 inflammasome activation. Nature 2011;469:221–225.
[32] Hanahan D, Weinberg RA. Hallmarks of cancer: the next generation. Cell 2011;144:646–674.
[33] Takehara T, Liu X, Fujimoto J, Friedman S, Takahashi H. Expression and role of Bcl-xL in human hepatocellular carcinomas. Hepatology 2001;34:55–61.
[34] Fleischer B, Schulze-Bergkamen H, Schuchmann M, Weber A, Biesterfeld S, Müller M, et al. Mcl-1 is an anti-apoptotic factor for human hepatocellular carcinoma. Int J Oncol 2006;28:25–32.
[35] Sieghart W, Losert D, Strommer S, Cejka D, Schmid K, Rasoul-Rockenschaub S, et al. Mcl-1 overexpression in hepatocellular carcinoma: a potential target for antisense therapy. J Hepatol 2006;44:151–157.
[36] Watanabe J, Kushihata F, Honda K, Sugita A, Tateishi N, Mominoki K, et al. Prognostic significance of Bcl-xL in human hepatocellular carcinoma. Surgery 2004;135:604–612.
[37] Hikita H, Takehara T, Shimizu S, Kodama T, Shigekawa M, Iwase K, et al. The Bcl-xL inhibitor, ABT-737, efficiently induces apoptosis and suppresses

growth of hepatoma cells in combination with sorafenib. Hepatology 2010;52:1310–1321.
[38] Chen CF, Lee WC, Yang HI, Chang HC, Jen CL, Iloeje UH, et al. Changes in serum levels of HBV DNA and alanine aminotransferase determine risk for hepatocellular carcinoma. Gastroenterology 2011;141:1240–1248.
[39] Bhala N, Angulo P, van der Poorten D, Lee E, Hui JM, Saracco G, et al. The natural history of nonalcoholic fatty liver disease with advanced fibrosis or cirrhosis: an international collaborative study. Hepatology 2011;54:1208–1216.
[40] Ruhl CE, Everhart JE. Elevated serum alanine aminotransferase and gamma-glutamyltransferase and mortality in the United States population. Gastroenterology 2009;136:477–485, e411.
[41] Pockros P, Schiff E, Shiffman M, McHutchison J, Gish R, Afdhal N, et al. Oral IDN-6556, an antiapoptotic caspase inhibitor, may lower aminotransferase activity in patients with chronic hepatitis C. Hepatology 2007;46:324–329.

IJC
International Journal of Cancer

Suppression of signal transducers and activators of transcription 1 in hepatocellular carcinoma is associated with tumor progression

Atsushi Hosui[1], Peter Klover[2], Tomohide Tatsumi[1], Akio Uemura[1], Hiroaki Nagano[3], Yuichiro Doki[3], Masaki Mori[3], Naoki Hiramatsu[1], Tatsuya Kanto[1], Lothar Hennighausen[2], Norio Hayashi[4] and Tetsuo Takehara[1]

[1] Department of Gastroenterology and Hepatology, Osaka University Graduate School of Medicine, 2-2 Yamadaoka, Suita, Osaka, Japan
[2] Laboratory of Genetics and Physiology, National Institute of Diabetes and Digestive and Kidney Diseases, National Institutes of Health, Bethesda, MD
[3] Department of Surgery, Osaka University Graduate School of Medicine, 2-2 Yamadaoka, Suita, Osaka, Japan
[4] Kansai-Rosai Hospital, 3-1-69, Inabaso, Amagasaki, Hyogo, Japan

Signal transducers and activators of transcription (STAT) 1 plays a pivotal role in cell-cycle and cell-fate determination, and vascular endothelial growth factor (VEGF) also contributes tumor growth. Recently, interferon (IFN) α has been reported to be effective for prevention of hepatocellular carcinomas (HCCs) recurrence, but the detailed mechanisms remain elusive. *In vitro*, cobalt chloride–treated VEGF induction and hypoxia responsive element (HRE) promoter activity were inhibited by IFNs and this abrogation was cancelled by introduction of small interfering RNA for STAT1. Immunoprecipitation/chromatin immunoprecipitation analyses showed STAT1 bound to hypoxia-inducible factor (HIF)-1α and dissociated HIF-complex from HRE promoter lesion. In a xenograft model using Balb/c nude mice, tumor growth was suppressed by IFNα through inhibition of VEGF expression and it was oppositely enhanced when STAT1-deleted cells were injected. This augmentation was due to upregulation of VEGF and hyaluronan synthase 2. In human samples, 29 HCCs were resected, divided into two groups based on STAT1 activation in tumor and the clinical features were investigated. Patients with suppressed STAT1 activity had a shorter recurrence-free survival. Histological and reverse transcriptase-polymerase chain reaction (RT-PCR) analyses showed portal vein microinvasion and increased VEGF levels in tumors from suppressed STAT1 group. These human samples also showed a reverse correlation between VEGF and STAT1-regulated genes expression. These results *in vitro* and *in vivo* suggested that IFNα are potential candidates for prevention of vessel invasion acting through inhibition of VEGF expression and need to be properly used when STAT1 expression is suppressed.

Key words: STAT1, VEGF, HCC, HIF-1, IFNα

Abbreviations: CH: chronic hepatitis; ChIP: chromatin immunoprecipitation; CoCl2: cobalt chloride; FGF: fibroblast growth factor; HAS: hyaluronan synthase; HCC: hepatocellular carcinoma; HIF: hypoxia-inducible factor; HRE: hypoxia responsive element; IFN: interferon; Ip: Immunoprecipitation; IP: intraperitoneally; IRF: interferon regulatory factor; JAK: Janus kinase; LC: liver cirrhosis; MMP: matrix metalloproteinase; multi: multiple nodular type; NT: adjacent non-tumor tissue; pSTAT: phosphorylated STAT; simple: simple nodular type; STAT: signal transducers and activators of transcription; surr: simple nodule with surrounded proliferation; T: HCC tumors; TIMP: tissue inhibitor of metalloproteinase; TK: thymidine kinase; VEGF: vascular endothelial growth factor
Additional Supporting Information may be found in the online version of this article.

Grant sponsor: Ministry of Education, Culture, Sports, Science, and Technology, Japan
DOI: 10.1002/ijc.27580
History: Received 9 Sep 2011; Accepted 20 Mar 2012; Online 5 Apr 2012

Correspondence to: Tetsuo Takehara, Department of Gastroenterology and Hepatology, Osaka University Graduate School of Medicine, 2-2 Yamadaoka, Suita, Osaka 565-0871, Japan, Tel.: [(81)-6-6879-3621], Fax: +[81-6-6879-3629], E-mail: takehara@gh.med.osaka-u.ac.jp

Introduction

Hepatocellular carcinoma (HCC) is a very common malignancy and causes more than six hundred thousand patients' deaths annually worldwide. The prognosis of HCC is still poor because it often develops with vessel invasion. Several studies have revealed that neovascularization and angiogenic factors, such as vascular endothelial growth factor (VEGF), are significantly upregulated in human HCC samples and play a considerable role in its development and progression.[1]

VEGF contributes to completing vessel invasion and distant metastasis because angiogenesis is thought to be essential for tumor growth. In addition, it is thought that cancer tissues with abundant tumor vessels have many routes of access to distant organs. We are interested not only in the angiogenic potential of VEGF but also in its permeability potential. The permeability function of VEGF appears to strongly involve cancer invasion and metastasis, because high permeability leads to the fragility and opening of cell-to-cell adherence in the vascular endothelium, which might allow the cancer cells to migrate into the vascular lumen.[2]

Interferon (IFN) therapy is frequently used for eradication of hepatitis C virus (HCV) and recently for prevention of HCC recurrence. IFNs are a superfamily of proteins secreted

by human cells that manifest multiple functions in the human body such as protection of cells from viral infection, regulation of cell growth and modulation of the immune system. There are two types of IFN, type 1 IFN (IFNα/β) and type II IFN (IFNγ). The roles of these IFNs against tumor progression and invasion have been reported by several investigators. IFNα inhibits VEGF expression and tumor angiogenesis in neuroendocrine tumors.[3] Qin et al. showed that IFNγ downregulates matrix metalloproteinase (MMP) 2, and Singh et al. presented results showing that IFNα suppresses fibroblast growth factor 2 (FGF2).[4,5] As for signal transducers and activators of transcription (STAT) 1, which is activated by IFNs, genetic polymorphisms in STAT1 gene is reported to associate with increased risk of HCC.[6] In a clinical setting, however, it remains unclear whether and how IFN-STAT signal transduction is associated with tumor progression and vessel invasion. In this study, we investigated the role of IFN-STAT signaling in the process of HCC tumor development using a combination of clinical HCC samples, several HCC cell lines and tumor-transplanted nude mice.

Material and Methods

Cell lines and tissues

Human hepatoma cell lines, PLC/PRF/5, Huh7 and HepG2, were purchased from American Type Culture Collection approximately 3 years ago, and have been tested every year to confirm that their sequences were conserved. They were cultured with Dulbecco's modified Eagle medium supplemented with 10% heat-inactivated fetal bovine serum and treated with various concentrations of IFNα (R&D systems, Minneapolis, MN)/γ (Hayashibara Group, Japan) and/or 100 mM of cobalt chloride ($CoCl_2$; Sigma) and/or 100 ng/ml of IL-6 (R&D systems) or exposed to hypoxia (1% O_2 condition), and then extracted 24 hr after stimulation. To block Janus kinase (JAK)-STAT signal transduction, 100 nM of JAK inhibitor 1, a broad inhibitor of JAKs (Calbiochem, Darmstadt, Germany) or S31-201, specific STAT3 inhibitor (Selleck, TX) was pretreated 1 hr before stimulation. For detection of hydroxylated-hypoxia-inducible factor (HIF)-1α, cells were extracted with lysate buffer including 10 μM of MG132 (Sigma). HCCs and adjacent non-tumor (NT) counterparts were obtained at the time of surgical resection. Written informed consent was provided from each patient. We also obtained the approval of the Ethics committee in Osaka University Graduate School of Medicine.

Plasmid constructs

The pGL2TK plasmid was generated by replacing the SV40 promoter of pGL2 promoter (Promega) with the herpes simplex virus thymidine kinase (TK) promoter fragment (from −105 to +51). The pGL2TkHRE plasmid was kindly provided by Uranchimeg B, National Cancer Institute. In brief, it was produced by subcloning three copies of the HRE (5′-GTGACTACGTGCTGCCTAG-3′) from the iNOS promoter into the pGL2TK promoter vector.[7]

Mice

Balb/c nude mice (CAnN.Cg-Foxn1^{nu}/CrlCrlj) were purchased from Charles River Laboratories (Yokohama, Japan). They were maintained in a specific pathogen-free facility and treated with humane care with approval from the Animal Care and Use Committee of Osaka University Medical School.

Xenograft tumor

To produce a xenograft tumor, 5×10^6 PLC/PRF/5 cells were subcutaneously injected to Balb/c nude mice. For anticancer therapy, 5×10^4 IU/mouse of human IFNα was administrated intraperitoneally (IP) every day, and the same volume of 0.9% saline was injected as a control. Treatment with 10 μg/g BW of bevacizumab (Chugai Pharmaceutical, Japan) IP was started 3 days after injection of HCC cells and was continued three times a week.

Immunoblotting and immunostaining

For immunoblotting, total cellular protein was electrophoretically separated by sodium dodecyl sulfate polyacrylamide gels and transferred onto polyvinylidene difluoride (PVDF) membrane. The membrane was blocked in Tris-buffered saline-Tween containing 5% skim milk for 1 hr and then probed with primary Antibody (Ab) at 4°C overnight. Rabbit monoclonal anti-pSTAT1/STAT1/HIF-1α/hydroxylated HIF-1α Abs and mouse monoclonal anti-STAT3/pSTAT3 Abs were purchased from Cell SignalingTechnology (Beverly, MA). Mouse monoclonal anti-VEGF Ab was from Calbiochem, and anti-CD31 Ab was from R&D systems. Mouse polyclonal anti-β-actin was obtained from Sigma. Horseradish peroxidase-conjugated anti-rabbit or mouse Ab and SuperSignal West Pico System (Pierce, Rockford, IL) were used for the detection of blots.

For immunohistochemistry, tumors were excised and prepared for immunostaining. Tumors were consecutively incubated in PBST for 15 min, in blocking buffer [phosphate-buffered saline with Tween 20 (PBST), 5% normal goat serum, 0.2% bovine serum albumin] for 30 min, in anti-CD31 Ab in blocking buffer for 12 hr, in PBST for 15 min, in Alexa fluor 594 (Molecular Probes, NY) in blocking buffer for an hour, and in PBST for 30 min. Finally, a coverslip was mounted in the mounting medium (Vectashield, Vector Laboratories) with 4′,6-diamidino-2′-phenylindole-dihydrochrolide, and the cells were examined by microscopy.

Protein–protein interaction analysis

To examine the binding of STAT1 protein to HIF-1α protein, immunoprecipitation/western blot analyses were used. The detail procedure is described elsewhere.[8] In brief, from $CoCl_2$ and IFNγ-treated PLC/PRF/5 cells, the cellular protein was extracted and precleared by incubation with protein A-Sepharose beads at 4°C for 1 hr. Next, the sample was incubated with beads coupled to STAT1, pSTAT1, HIF-1α, or hydroxylated-HIF-1α antibody, or rabbit nonspecific γ-globulin (Dako, Denmark) for 18 hr. The immune complex was

eluted by being boiled for 5 min, and finally the supernatant was used for western blot to detect each protein.

Analyses of cell growth

To examine the cell growth curve, 5×10^3 of PLC/PRF/5 cells were seeded on a 96-well culture plate. After 24, 48, 72 and 96 hr, the net number of viable cells was assessed colorimetrically using water-soluble tetrazolium (2-[2-methoxy-4-nitrophenyl]-3-[4-nitrophenyl]-5-[2,4-disulfophenyl]-2*H*-tetrazolium monosodium salt) (Roche Applied Science, IN). This assay is based on cleavage of the tetrazolium salt by mitochondrial dehydrogenase in viable cells. For the assay, 10 μl of the water-soluble tetrazolium reagent was added to the 100-μl culture medium, followed by the incubation at 37°C for 1 hr. The optical density at 450 nm was measured. The assay was done in quadruplicate and the values were expressed as the means ± S.D.

ChIP

Chromatin immunoprecipitation (ChIP) analysis was basically performed according to the manufacturers' instructions of MAGnify ChIP System (Invitrogen). In brief, cells (~5.0×10^7) were grown to a confluencey of 85–90% in complete media and treated with 100 μM $CoCl_2$ for 24 hr. These cells were treated with 1% formaldehyde for 10 min at room temperature, followed by the addition of 1.25 M glycine to a final concentration of 0.125 M. Cells were washed in 4°C PBS and pelleted in 1 ml of lysis buffer with protease inhibitors and incubated for 10 min at 4°C. Nuclear lysates were sonicated (Sonifier 250, Branson) for 15 cycles of 30 sec ON and 30 sec OFF to shear DNA to 200–500 bp fragments. Chromatin solutions were precleared and incubated with anti-HIF-1α, STAT1 or the nonspecific γ-globulin (negative control) and rotated overnight at 4°C. Chromatin/protein complex was purified and applied to PCR analysis. The region −1,386 to −1,036 of the VEGF promoter was PCR amplified from the immunoprecipitated chromatin using the following primers: sense 5′-CAGGTCAGAAACCAGCCAG, antisense; 5′-CGTG ATGATTCAAACCTACC. The 350-bp PCR product was resolved on a 1.2% agarose gel and visualized by ethidium bromide staining and UV illumination.

RNA extraction, real-time PCR analysis and small RNA interference

Total RNA was isolated (miRNeasy Mini Kit, Qiagen, Valencia, CA), reverse-transcribed (High Capacity RNA-to-cDNA Master Mix, Applied Biosystems) and then applied to real-time PCR analysis (TaqMan Gene Expression Assays, Applied Biosystems) normalized to beta-actin expression levels. All measurements were performed in triplicate. The details of each probe for real-time PCR are described in Table 1, Supporting Information. Cells were transfected with Stealth select RNA interference (RNAi, set of three oligonucleotides, Invitrogen) directed against STAT1. A Stealth RNAi negative control kit (set of three oligonucleotides, Invitrogen) was used as a control for sequence-independent effects following Stealth RNAi delivery. The transfections were carried out using Lipofectamine RNAiMAX (Invitrogen) according to the reverse transfection protocol.

Quantitative analysis of hyaluronic acid

Hyaluronic acid enzyme-linked immunosorbant assay (ELISA) kit was purchased from Biotech Trading Partners (NY). Each assay was performed according to the manufacturer's instructions. In brief, the removed subcutaneous tumors were dried and treated with pronase E for 24 hr. The product was boiled for 10 min and centrifuged, and the supernatants were subjected to ELISA assay.

Statistical analysis

Data were presented as mean ± standard error (SE) (for *in vivo* experiments) or as mean ± standard deviation (for *in vitro* experiments). Comparisons between the two groups were performed by the unpaired *t*-test. Multiple comparisons were performed by ANOVA with the Scheffe post hoc test. Recurrence-free survival curves were estimated using the Kaplan-Meier method. $p < 0.05$ was considered statistically significant.

Results

IFNα suppresses VEGF expression through inhibiting HRE-promoter activity

To clarify the relationship between STAT1 activity and VEGF expression in HCC, we used a hypoxia model to induce VEGF expression, and treated HCC cell lines with IFNα, which is known to activate STAT1.[9] This hypoxia model mimics the clinical setting of HCC, which was done by administration of $CoCl_2$. Our results shown in Figure 1*a* were compatible with previous reports, suggesting that both $CoCl_2$ and IFNα worked well in this experiment using PLC/PRF/5 cells. VEGF mRNA/protein expression was enhanced by $CoCl_2$, but this induction was inhibited by IFNα administration in a dose-dependent manner. This inhibitory effect was cancelled by introduction of JAK inhibitor or STAT1 knockdown (Figs. 1*b* and 1*c*). HepG2 and Huh7 cells were both used and displayed the same tendencies as these results (Fig. 1, Supporting Information). VEGF expression is regulated by the heterodimeric HIF-1, which is made up of HIF-1α and HIF-1β to the hypoxia responsive elements (HRE) on several target genes. HIF-1β is constitutively expressed irrespective of various conditions, but HIF-1α is proline-hydroxylated leading to a conformational change that promotes ubiquitination and proteasomal degradation under normoxic conditions.[10] We next tried to find how $CoCl_2$-induced VEGF induction was suppressed by IFNα stimulation by examining the expression levels of HIF-1α and hydroxylated HIF-1α. $CoCl_2$ induced HIF-1α expression, and this induction level was not altered by IFNα treatment (Fig. 1*d*). Hydroxylated HIF-1α was expressed at low levels with or without $CoCl_2$ and/or IFNα. This inhibitory effect of

Table 1. Demographic characteristics of patients and tumors

	Total HCC patients	Suppressed pSTAT1 group	control group
Total number	29	7	22
Male/Female	21/8	6/1	15/7
Age (year)	61.6 ± 10.3	66.5 ± 8.0	60.2 ± 10.8
Etiology (HBV/HCV)	11/15	3/5	8/10
NT lesion (normal/CH/LC)	2/18/9	0/6/1	2/12/8
ALT	44.0 ± 30.0	41.1 ± 21.0	46.2 ± 33.2
Platelets	15.7 ± 5.8	14.7 ± 1.9	16.0 ± 5.6
Child (A/B/C)	20/3/6	7/0/0	13/3/6
Stage (I/II/III/IV)	2/16/10/1	0/6/1/0	2/10/9/1
HCC recurrence (within/over 2 years)	15/14	7/0 *1	8/14
Tumor size (cm)	4.8 ± 2.6	5.5 ± 2.4	4.6 ± 2.3
Macroscopic classification (simple/surr/multi/invasive)	6/13/6/4	1/5/0/1	5/8/6/3
Capsule formation (+/−)	20/9	7/0 *2	13/9
Histology (moderate/poor)	10/19	3/4	7/15
AFP	1337 ± 4402	766 ± 579	1637 ± 5161
Vessel invasion (Vv +/−)	1/28	0/7	1/21
Vessel invasion (Vp +/−)	9/20	5/2 *3	4/18

Liver function was categorized by Child-Pugh classification and the tumors were also staged by means of the pTNM system. At least every 3 months, diagnostic imaging and blood sampling was done to check for HCC recurrence. Asterisks indicate significant differences (*1, $p = 0.0033$, *2, $p = 0.042$, *3, $p = 0.008$).

IFNα on VEGF expression was also seen in low O_2 condition (Fig. 2, Supporting Information). Next, HRE promoter activity was assessed by transfection of the luciferase construct (pGL2TkHRE) that included HRE and the minimal promoter TK gene upstream of the luciferase gene.[7,11] As shown in Figure 1*e*, HRE promoter activity was enhanced by treatment with $CoCl_2$, and this upregulation was inhibited by IFNα stimulation. This inhibitory effect was abolished by introducing STAT1 siRNA as is the case with VEGF expression. IFNγ has also the same inhibitory effect on VEGF expression as IFNα (Fig. 3, Supporting Information). Our results, therefore, show that activation of JAK-STAT1 signal transduction causes inhibition of VEGF expression through suppression of HRE promoter activity.

STAT1 forms a complex with HIF-1α

We hypothesized that a direct interaction of STAT1 and HIF-1 could be responsible for the effect of pSTAT1 on formation of the HIF-1 complex or on its binding to HRE. To test this, we examined the binding of STAT1 to HIF-1 protein by means of immunoprecipitation (Ip)/western blot analysis (Fig. 1*f*). From $CoCl_2$ and IFNγ-treated PLC/PRF/5 cells, the cellular protein was extracted and applied to Ip assay. The HIF-1α protein was not found in the negative control using nonspecific γ-globulin (*lane 1*) but detected in the immunoprecipitates using antibodies against pSTAT1 (*lane 2*) and STAT1 (*lane 3*). In similar fashion, STAT1 protein was seen in the immunoprecipitates using antibodies against HIF-1α. These findings indicate the possible binding of HIF-1α protein to STAT1 protein. To further determine if this interaction has an effect on binding of the HIF-1 complex to HRE, we performed *in vitro* ChIP assays. Cultured cells were treated with $CoCl_2$ in the absence (Fig. 1*g*, *lanes 1, 4*) or presence of IFNγ (*lanes 2, 5*). Before these treatments, STAT1 expression was knocked down by siRNA (*lanes 3, 6*). The PCR product designed within HRE was not found in the negative control sample using nonspecific γ-globulin (*lanes 1-3*) but detected in the immunoprecipitates using antibodies against HIF-1α (*lanes 4-6*). The detection level was less in IFNα-treated cells, and this inhibitory effect was canceled in STAT1-deleted cells. No bands were seen in immunoprecipitates using STAT1 antibodies (lane 7) though STAT1 binds to HIF-1α complex and then might be associated with HRE. These results indicate that STAT1 bound to HIF-1α protein, and this binding caused the HIF-1α complex disassociate with HRE.

IFNα has an inhibitory effect on tumor development in the presence of STAT1 but an opposite effect in the absence of STAT1

Several investigators have already reported that IFNα has antiproliferative effects by inhibiting cell-cycle progression or by inducing apoptosis.[12,13] *In vitro*, the growth of cultured cells were inhibited by IFNα stimulation irrespective of STAT1, indicating that antiproliferative effects involve both STAT1-dependent and -independent mechanisms (Fig. 4, Supporting Information). To clarify the relationship between IFNα-STAT1 and VEGF *in vivo*, we developed a xenograft model using nude mice. STAT1 gene knock down by siRNA

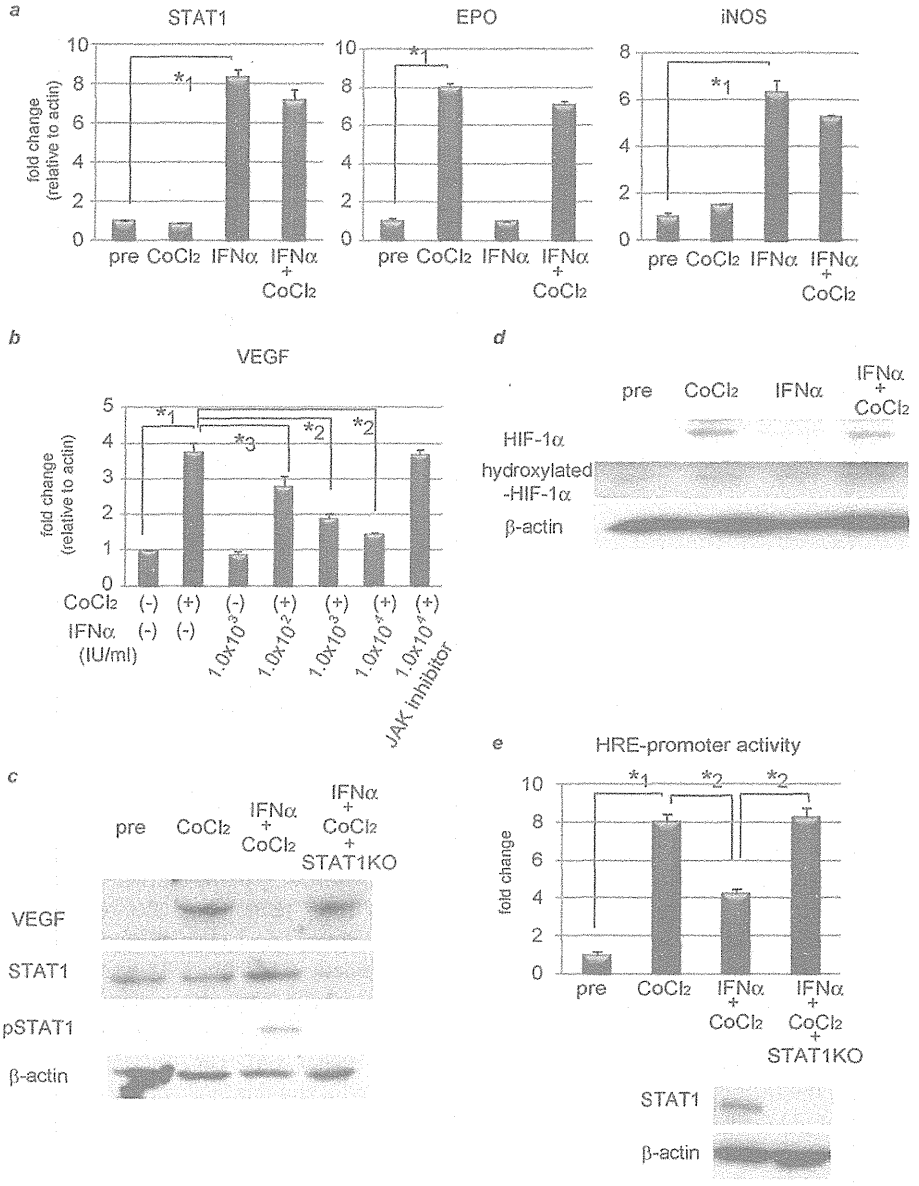

Figure 1. IFNα suppresses VEGF expression through inhibiting HRE-promoter activity by interaction between STAT1 and HIF-1 complex. (*a*, *b*) Expression levels as detected by real-time RT-PCR analysis. Cells were treated with 100 μM $CoCl_2$ and/or 1.0×10^3 IU/ml (*a*) or various concentrations of IFNα (*b*) for 24 hr. To block JAK-STAT signal transduction, 100 nM of JAK inhibitor 1 was pretreated 1 hr before stimulation. (*c*) Activation of STAT1 and expression of STAT1 and VEGF as detected by western blot analysis. PLC/PRF/5 cells were transfected with control siRNA or siRNA for STAT1 and subjected to each stimulation for 24 hr. (*d*) Expression levels of HIF-1α and hydroxylated-HIF-1α as detected by western blot analysis. (*e*) Cells were cotransfected of the pGL2TkHRE plasmid or the pGL2Tk plasmid (as a control vector) with the pRLtK plasmid (Promega). The cells were then stimulated with 100 mM of $CoCl_2$ units/ml and/or 1.0×10^3 IU/ml of IFNα, or left unstimulated, and subjected to dual luciferase assay. The relative light unit of the unstimulated sample was considered as 1 and the data were expressed as mean ± S.D. Lower panel shows expression levels of STAT1 as detected by western blot analysis. (*f*) Cellular lysates from $CoCl_2$ and IFNγ-treated PLC/PRF/5 cells were immunoprecipitated with nonspecific γ-globulin (*lane 1*) and antibodies against pSTAT1 (left panel, *lane 2*), STAT1 (left panel, *lane 3*), HIF-1α (right panel, *lane 2*), and hydroxylated-HIF-1α (right panel, *lane 3*), and the immunoprecipitates were subjected to western blot analysis to detect each protein. (*g*) ChIP assay with HIF1α or STAT1 antibody. Cells were transfected with siRNA for STAT1 or control, and stimulated with $CoCl_2$ for 24 hr and/or IFNα for 3 hr. The immunoprecipitated DNA was purified and the region from −1386 to −1036 base pairs of the human VEGF promoter was amplified by PCR (35 cycles). Cell lysates without Ip was used as a positive control (lane 8). Asterisks indicate significant differences (*1, $p < 0.001$, *2, $p < 0.01$, *3, $p < 0.05$).

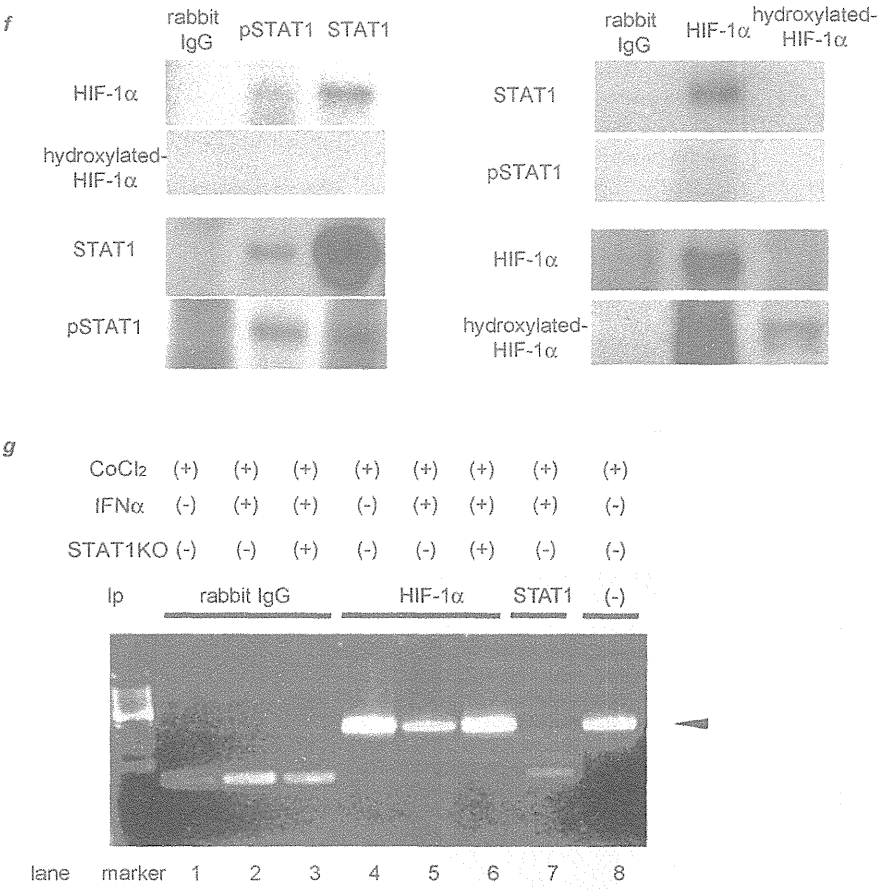

Figure 1. (Continued)

was tested for reduction of STAT1 levels in several hepatoma cell lines. Western blot analysis showed STAT1 expression had been reduced by this method for more than 20 days, and that it was most efficient in PLC/PRF/5 cells (Fig. 5, Supporting Information). Several nude mice were then subcutaneously injected with control and STAT1-deleted cells to form xenograft tumors and were randomly assigned into two groups; one was treated with human IFNα, and the other with 0.9% saline as the control. In the presence of STAT1, IFNα had a strong inhibitory effect on the tumor development as expected, but in the absence of STAT1, surprisingly, IFNα had the opposite effect, that is, it enhanced tumor growth (Fig. 2*a*). Without IFNα treatment, there was no significant difference in tumor growth between control and STAT1-deleted cells. We also confirmed that STAT1 expression in tumor had been knocked down for at least 20 days after injection (Fig. 2*b*). Real-time RT-PCR and western blot analyses revealed that VEGF expression in tumors resected 20 days after transplantation was lower in the IFNα-treated group than in the control, which was consistent with the *in vitro* results, but surprisingly it was increased when the STAT1 gene was knocked down (Figs. 2*c* and 2*d*). To examine whether inhibition or progression of tumor growth was due to VEGF levels, we used bevacizumab, a VEGF monoclonal antibody, and measured tumor size at 25 days after injection of tumor cells. No differences were noted between the control and IFNα-treated groups irrespective of STAT1 expression when these mice were treated with bevacizumab (Fig. 2*e*). To examine the possibility that the human IFNα acts *in vivo* equally well on mouse cells and on human cell lines, we extracted mouse liver as well as transplanted tumor and examined STAT1 activity. It revealed that STAT1 was strongly activated in human cell lines but less activated in mouse liver (Fig. 6, Supporting Information). These data suggest that in this model, IFNα had an inhibitory effect on tumor growth through inhibition of VEGF expression, and that it also had a promotive effect through enhancement of VEGF expression when STAT1 expression was knocked down in tumor cells.

As a typical hypervascular tumor, HCC produces and secretes VEGF, thereby forming new tumor vessels, which provide oxygen and nutrients to cancer cells causing them to grow. Microvessel density was assessed by CD31 immunostaining of hepatic tumors resected 25 days after injection of tumor cells. It revealed that the number of CD31 positive cells,

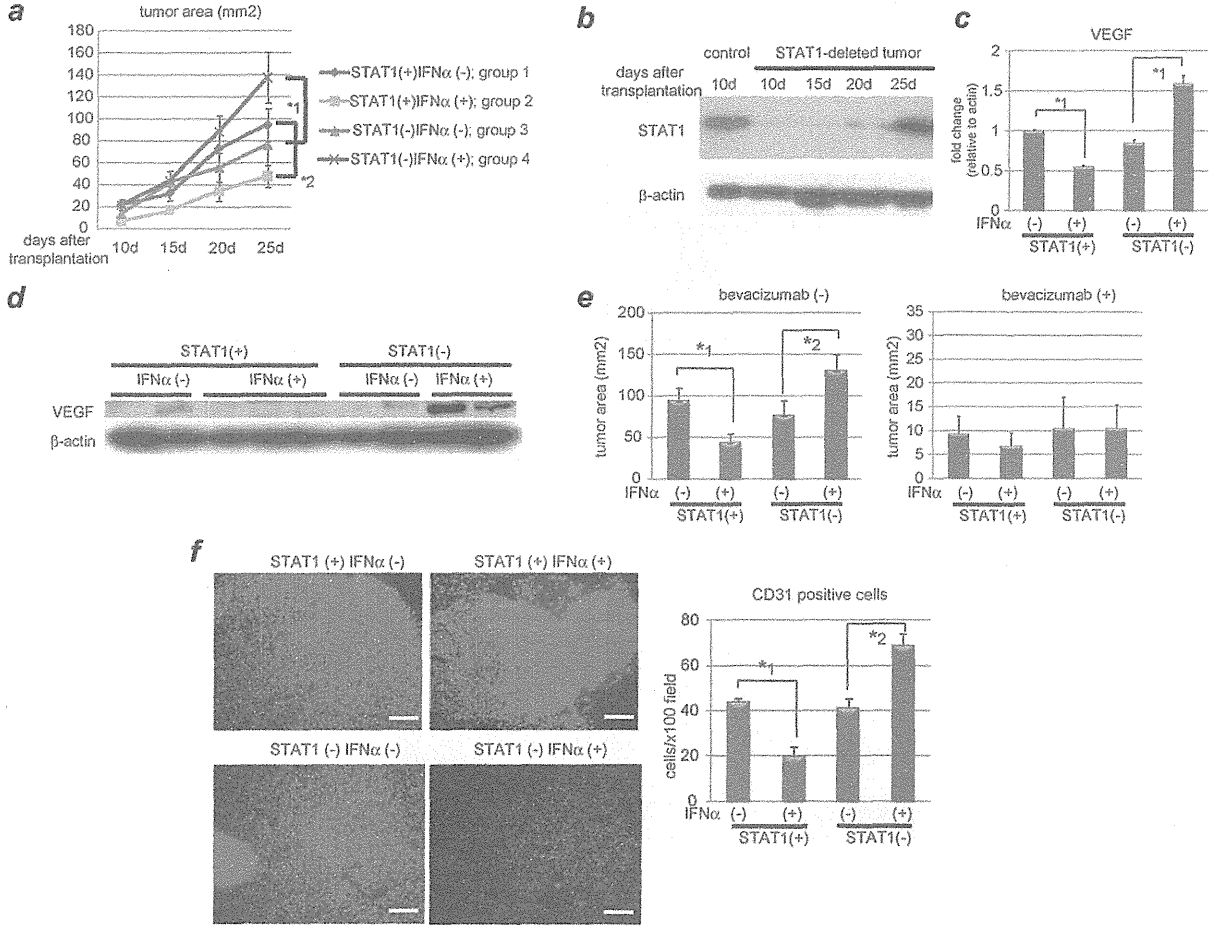

Figure 2. IFNα has an inhibitory effect on tumor development in the presence of STAT1 but an opposite effect in the absence of STAT1. (*a*) PLC/PRF/5 cells were transfected with control siRNA (group 1 and 2) or siRNA for STAT1 (group 3 and 4). One day after treatment, 5×10^6 of these cells were subcutaneously injected to Balb/c nude mice, and tumor area was measured every 5 days. In two groups (group 2 and 4), 5×10^4 IU/mouse of IFNα were administered IP every day, and in the other groups (group 1 and 3) the same volume of 0.9% saline was injected as a control. The number of mice in each group was 5–7. (*b*) Expression levels of STAT1 as detected by western blot analysis. Each subcutaneous tumor in group 4 was removed at the different time points (10, 15, 20 25 days after transplantation). One of tumors in group 2 was used as a positive control. (*c, d*) Expression levels of VEGF as detected by real-time RT-PCR or western blot analysis. Each subcutaneous tumor was removed 20 days after transplantation. (*e*) Tumor area at 25 days after transplantation in each group in the absence (left panel) or presence (right panel) of bevacizumab, the monoclonal anti-VEGF antibody ($N = 5–7$ per group). Three days after injection of tumor cells, 10 mg/g body weight of bevacizumab were injected IP twice a week. (*f*) Immunofluorescent staining with anti-CD31 (red) antibody and Dapi (blue). Images are shown at low magnification (100×, left panel). Bars, 200 μm. The number of CD31-positive cells were presented (right panel). These data were acquired from three different fields in each tumor. Asterisks indicate significant differences (*1, $p < 0.01$, *2, $p < 0.05$).

as an indicator of microvessels, was less in IFNα-treated mice, but without STAT1 they were enhanced by IFNα administration (Fig. 2*f*). Taken together, IFNα plays contrary roles for forming tumor vessels by regulating VEGF expression.

IFNα regulates VEGF expression through STAT3 activation in STAT1-null cells

Tumor growth was seen only in the STAT1-deleted and IFNα-treated group even when 1×10^5 cells were injected, although no tumors were observed in the other groups (Fig. 3*a*). Some adhesion molecules were examined and hyaluronan synthase (HAS) 2 was induced by IFNα stimulation in the STAT1-deleted cells and higher expression levels of hyaluronic acid were observed in the STAT1-deleted and IFNα-treated tumors (Figs. 3*b* and 3*c* and Fig. 7, Supporting Information). The presence of STAT1 has an effect on them because HAS2 expression and HA concentration were also different between STAT1 (+);IFN (−) group and STAT1(−); IFN (−) group. These results indicate that IFNα-STAT1 regulates HAS2 expression, promoting attachment of tumor cells, because HAS2 has been implicated in the developmental process involving adherence to the extracellular matrix

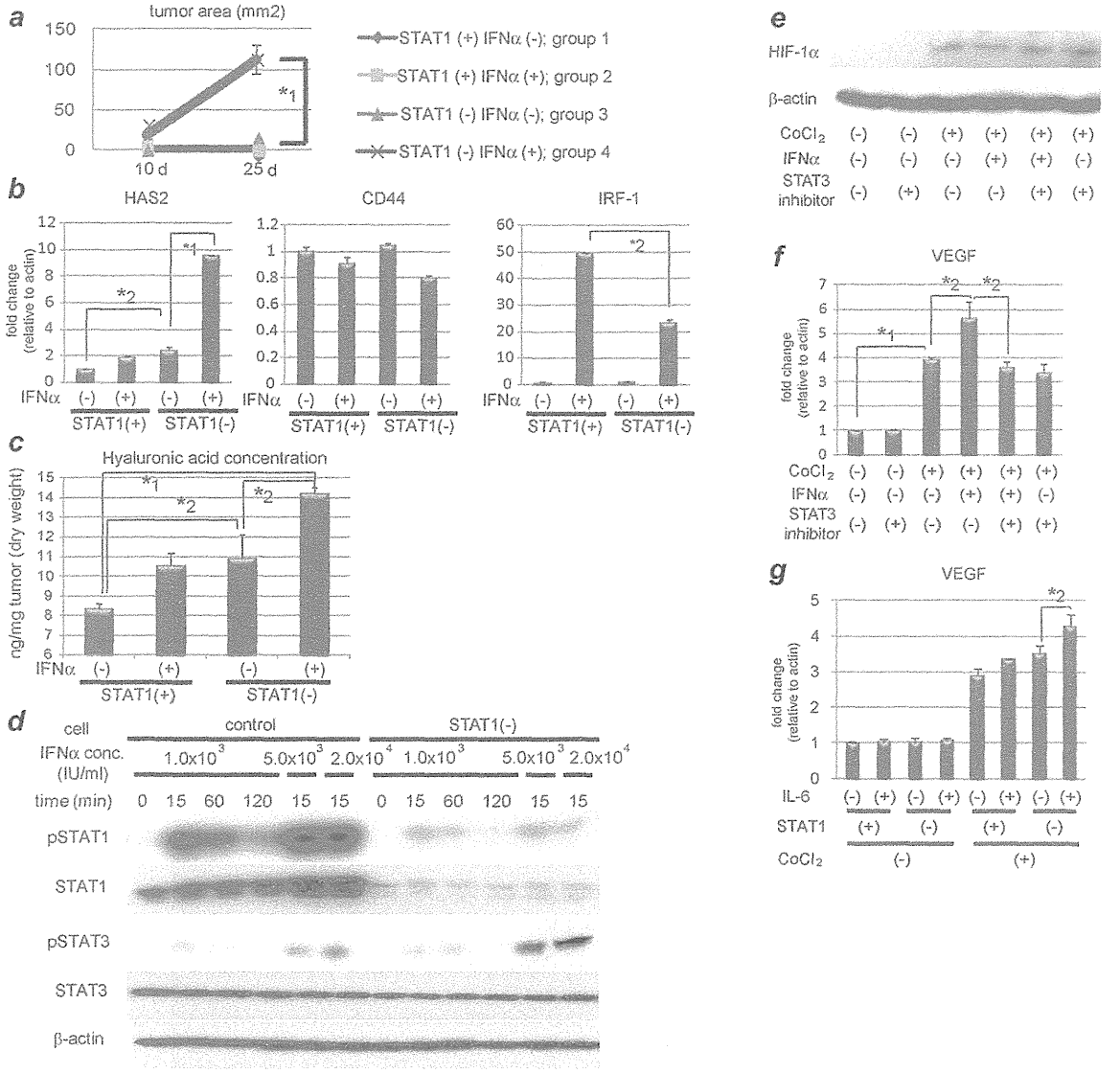

Figure 3. IFNα causes enhancement of HAS2 and VEGF through STAT3 activation in the absence of STAT1. (*a*) 1×10^5 of transfected cells were subcutaneously injected to Balb/c nude mice. Other procedures are the same as *b*. (*b*) Expression levels of hyaluronic acid synthase (HAS) 2, CD44 and IRF-1 as detected by real-time RT-PCR analysis. PLC/PRF/5 cells were transfected with control siRNA or siRNA for STAT1 and stimulated on the next day with 5.0×10^3 IU/ml of IFNα for 3 hr or left untreated. (*c*) Hyaluronic acid levels of each tumor as detected by ELISA assay. (*d*) Activation/expression of STAT1 and STAT3 as detected by western blot analysis. PLC/PRF/5 cells were transfected with control siRNA or siRNA for STAT1 and stimulated on the next day with various concentration of IFNα for 15, 60, or 120 min. (*e*, *f*) STAT1-knockdown cells were pretreated with or without 100 μM of S31-201, a specific STAT3 inhibitor, before $CoCl_2$ and/or 5.0×10^3 IU/ml of IFNα. (*e*) Expression levels of HIF-1α as detected by western blot analysis. (*f*, *g*) Expression levels of VEGF as detected by real-time RT-PCR analysis. (*g*) Control and STAT1-knockdown cells were treated with $CoCl_2$ and/or 100 ng/ml of IL-6. Asterisks indicate significant differences (*1, $p < 0.001$, *2, $p < 0.01$).

and tissue expansion through high expression of hyaluronic acid.[14]

The inhibitory effect of STAT1 on VEGF expression was due to its binding to HIF-1α, but the enhancement effect remains unclear. Jung et al.[15] have reported that STAT3 is a potential modulator of HIF-1-mediated VEGF expression. To examine STAT3 activation under IFNα stimulation, western blot analysis was performed. As shown in Figure 3*d*, 1.0×10^3 IU/ml of IFNα induced almost the same level of phosphorylated STAT3 (pSTAT3), but prolonged STAT3 activity more in the STAT1-deleted cells than in the control. Administration of a higher concentration of IFNα, such as 5.0×10^3 or 2.0×10^4 IU/ml, also caused much more activation of STAT3 in the STAT1 knock-down cells than in the control.

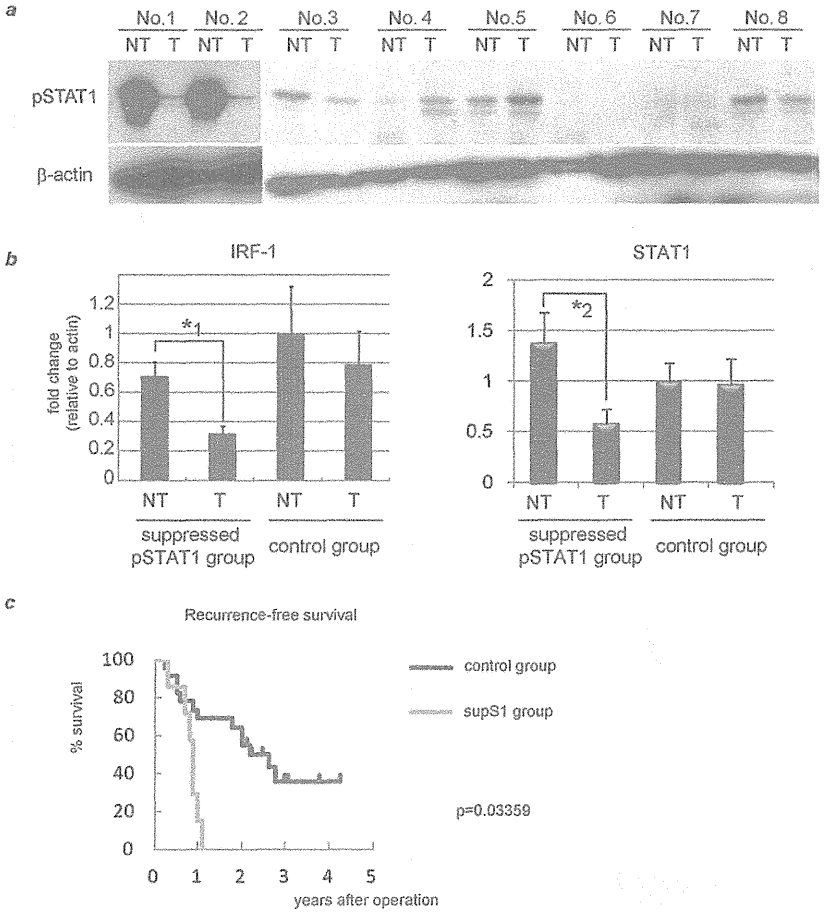

Figure 4. Suppressed STAT1 activity links to upregulation of VEGF, which might cause early HCC recurrence. Twenty-nine pairs of surgically resected human HCC tumors (T) and adjacent NT tissues were used. They were divided into two groups based on STAT1 activity (supS1 versus control). (*a*) Activation levels of STAT1 in T and NT as detected by western blot analysis. Representative data are presented. (*b, d*) Expression levels in each tissue of two divided groups as detected by real-time RT-PCR analysis. The relative expression level of the NT sample in the control group was set as 1, and the fold expression level of each tissue was calculated. (*c*) Predictors of recurrence-free survival were identified using the Kaplan-Meier method. (*e*) IRF-1, STAT1, and VEGF mRNA levels in the liver of 29 HCC samples were determined by real-time RT-PCR and plotted to analyze the correlation between IRF-1 and VEGF (Pearson correlation coefficient (R) = −0.5446, $p < 0.01$) (left) or between STAT1 and VEGF ($R = -0.5514$, $p < 0.01$) (right). The asterisks indicate significant differences (*1, $p < 0.01$, *2, $p < 0.05$, *3, $p < 0.05$ versus all other groups).

These data indicate that IFNα activated STAT3 without de novo protein synthesis, which might result in high expression of VEGF when STAT1 expression has been knocked down. The influence of enhanced STAT3 activity on HIF-1α expression in the STAT1 knock-down cells was examined by western blot analysis but IFNα had no effects on HIF-1α expression, irrespective of S31-201, specific STAT3 inhibitor (Selleck, TX)(Fig. 3*e*). Administration of $CoCl_2$ induced VEGF expression and this induction was enhanced by IFNα stimulation in STAT1-null cells (Fig. 3*f*). This augmentation was canceled by pretreatment with S31-201, providing evidence that IFNα enhanced VEGF expression through STAT3 activation in the absence of STAT1. This synergistic effect was found not only with $CoCl_2$ and IFNα stimulation, but also with $CoCl_2$ and IL-6 stimulation (Fig. 3*g*). These results indicate that inflammation itself is a potent modulator of VEGF expression when STAT1 expression is silenced or downregulated.

Patients with suppressed STAT1 activity show a poor prognosis, which might be linked to upregulation of VEGF

To examine the activity of STAT1 in human HCC samples, we used 29 pairs of surgically resected human HCC tumors (T) and adjacent NT tissue samples. The backgrounds of the 29 cases are shown in Table 1. No one had received radiation or chemotherapy after surgery. In seven cases, STAT1 phosphrylation was suppressed in T compared to NT while in two cases, it was enhanced. All cases were then divided into two groups. In suppressed STAT1 group, STAT1 activity level was reduced more than by two-fold in T to NT by

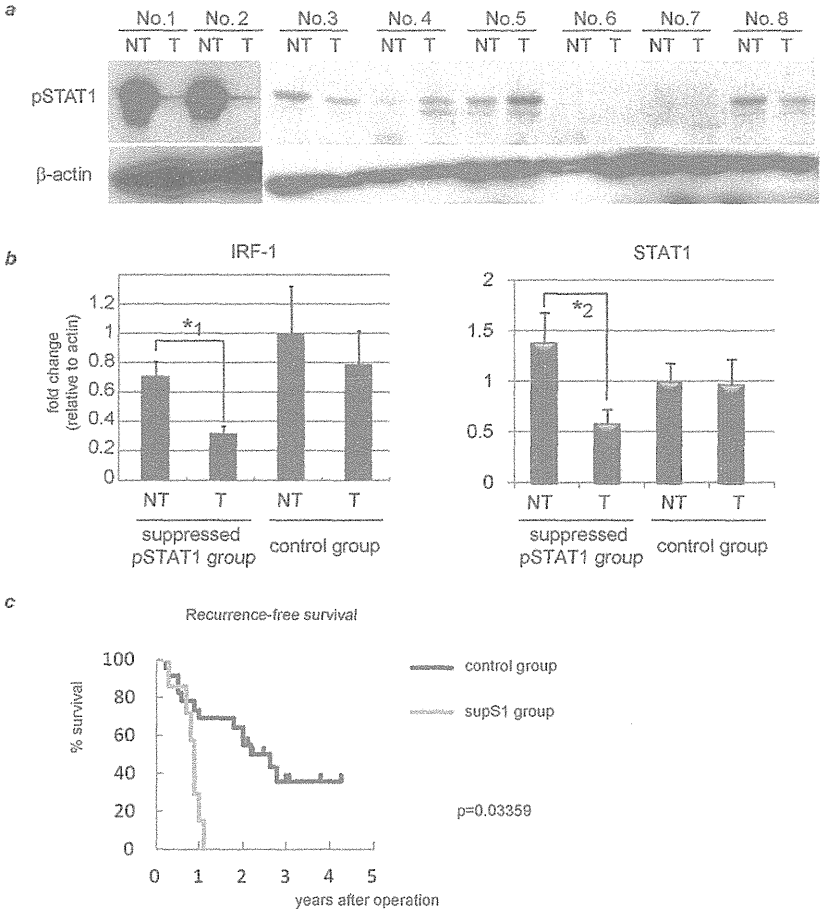

Figure 4. (Continued)

western blot (abbreviated as supS1 group, representative data was shown in Fig. 4*a*, No. 1 and 2). In 22 patients, STAT1 activation was not so changed or enhanced when comparing T with NT (control group, Fig. 4*a*, No. 3–8). These two groups had no statistical differences in their clinical backgrounds (Table 1). With most the same levels of serum alanine aminotransferase, our results suggest that these two groups had similar levels of hepatic inflammation. Expression of STAT1 target genes, such as interferon (IFN) regulatory factor (IRF)-1 and STAT1 itself, were measured by real-time RT-PCR, and statistically less expression of these molecules in the supS1 group were found in T than in NT (Fig. 4*b*). This is evidence for STAT1 activation in the supS1 group being suppressed in HCC tissues. Next, prognostic factors were examined, and surprisingly, all patients in the supS1 group displayed HCC recurrence within 2 years irrespective of having the same levels of liver function and staging of HCC compared to the control group (Table 1). We also observed suppression of STAT1 activity in tumor was associated with significantly worse recurrence-free survival by Kaplan-Meir analysis (Fig. 4*c*). As for the cause of the early recurrence in the supS1 group, the rate of microscopic portal venous invasion was significantly higher in the supS1 group. This finding indicates that the early recurrence may be associated with microportal invasion.

We next asked why suppression of hepatic STAT1 activity could be linked to vessel invasion by examining vessel invasion-related molecules, such as FGF, MMP, tissue inhibitor of metalloproteinase and VEGF, in these two subject groups. VEGF expression level was higher in the whole supS1 group than in the control, and its expression is much more enhanced in T than in NT (Fig. 4*d* and Fig. 8, Supporting Information). Other molecules were supposed not to contribute to the high HCC recurrence in supS1 group. Not only angiogenic potential but also permeability functions of VEGF appear to strongly mediate cancer invasion as described in the Introduction section.[2,16] These results and previous reports suggest that inhibited STAT1 activity might cause up-regulation of VEGF expression, resulting in portal invasion and poor prognosis.

To investigate finally the direct regulation of VEGF by STAT1 activation, we used these HCC samples. They

revealed a reverse correlation between VEGF and STAT1-regulated gene expression, such as IRF-1 and STAT1 itself (Fig. 4*e*). As the number of patients in this study was quite small, we cannot come to the strong conclusion, but these results are consistent with the hypothesis that STAT1 activation negatively regulates VEGF expression.

Discussion

Recently, IFNα therapy has been reported to be effective for preventing HCC recurrence.[17] IFN is known to exert immunomodulatory effects by stimulating T cells, natural killer cells and monocytes. These immune cells play roles in prevention of HCC recurrence by IFNα therapy, however, it remains elusive whether IFNα therapy is effective on hepatocytes, and how IFNα mediates its effect on them.

We have shown *in vitro* that IFNα-treated activation of JAK-STAT pathway causes inhibition of VEGF expression through abrogation of HRE-promoter activity. Some molecules were reported to have effects on gene transcription of VEGF,[3,18] but this is the first report to show that STAT1 directly binds to HIF-1 and regulates HRE-promoter activity. This is a newly discovered mechanism about IFNα-treated inhibition of VEGF expression, but more important is the fact that IFNα has adverse effects when STAT1 expression is silenced. That is, STAT3 is much more activated under stimulation with IFNα, followed by enhancement of expression of target genes, such as VEGF, as indicated in this study. This is the so-called "STAT-shift," and the same event occurs in the case of the growth hormone-STAT5, interleukin-6-STAT3.[19–21] STAT1 expression is regulated by IFNα, and thus the less activated the STAT1 is, the less it is expressed. This negative loop of STAT1 is more likely to occur in the clinical setting than other STATs. In some cases, IFNα therapy causes rapid progression of HCC with vessel invasion,[22] in which case the molecular pathogenesis might be explained by a STAT-shift and negative loop of STAT1 action.

This study has yielded three novel findings. First, patients with suppressed STAT1 activity have poor prognosis because of high HCC recurrence. This might be caused by upregulation of VEGF. Second, IFNα-treated activation of JAK-STAT pathway causes inhibition of VEGF expression through interaction of the HIF-1 complex with STAT1. Third, treatment with IFNα contributes to the harmful consequences when STAT1 expression is silenced or downregulated. These findings should be helpful for deciding which therapy is suitable for HCC patients. In some cases, conventional therapy should be replaced by other therapies, such as bevacizumab, one of the molecular target drugs for patients with suppressed STAT1 activity in tumor.

Acknowledgements

The authors are grateful to Badarch Uranchimeg (National Cancer Institute) for providing us with the pGL2TkHRE plasmid. They also thank Wei Li for technical assistance.

References

1. Mise M, Arii S, Higashituji H, et al. Clinical significance of vascular endothelial growth factor and basic fibroblast growth factor gene expression in liver tumor. *Hepatology* 1996;23:455–64.
2. Poon RT, Ng IO, Lau C, et al. Serum vascular endothelial growth factor predicts venous invasion in hepatocellular carcinoma: a prospective study. *Ann Surg* 2001;233:227–35.
3. von Marschall Z, Scholz A, Cramer T, et al. Effects of interferon alpha on vascular endothelial growth factor gene transcription and tumor angiogenesis. *J Natl Cancer Inst* 2003;95:437–48.
4. Qin H, Moellinger JD, Wells A, et al. Transcriptional suppression of matrix metalloproteinase-2 gene expression in human astroglioma cells by TNF-alpha and IFN-gamma. *J Immunol* 1998;161:6664–73.
5. Singh RK, Gutman M, Bucana CD, et al. Interferons alpha and beta down-regulate the expression of basic fibroblast growth factor in human carcinomas. *Proc Natl Acad Sci USA* 1995;92:4562–6.
6. Zhu ZZ, Di JZ, Gu WY, et al. Association of genetic polymorphisms in STAT1 gene with increased risk of hepatocellular carcinoma. *Oncology* 2011;78:382–8.
7. Rapisarda A, Uranchimeg B, Scudiero DA, et al. Identification of small molecule inhibitors of hypoxia-inducible factor 1 transcriptional activation pathway. *Cancer Res* 2002;62:4316–24.
8. Hosui A, Ohkawa K, Ishida H, et al. Hepatitis C virus core protein differently regulates the JAK-STAT signaling pathway under interleukin-6 and interferon-gamma stimuli. *J Biol Chem* 2003;278:28562–71.
9. Shuai K, Horvath CM, Huang LH, et al. Interferon activation of the transcription factor Stat91 involves dimerization through SH2-phosphotyrosyl peptide interactions. *Cell* 1994;76:821–8.
10. Maxwell PH, Wiesener MS, Chang GW, et al. The tumour suppressor protein VHL targets hypoxia-inducible factors for oxygen-dependent proteolysis. *Nature* 1999;399:271–5.
11. Melillo G, Musso T, Sica A, et al. A hypoxia-responsive element mediates a novel pathway of activation of the inducible nitric oxide synthase promoter. *J Exp Med* 1995;182:1683–93.
12. Yano H, Iemura A, Haramaki M, et al. Interferon alfa receptor expression and growth inhibition by interferon alfa in human liver cancer cell lines. *Hepatology* 1999;29:1708–17.
13. Dunn C, Brunetto M, Reynolds G, et al. Cytokines induced during chronic hepatitis B virus infection promote a pathway for NK cell-mediated liver damage. *J Exp Med* 2007;204:667–80.
14. Udabage L, Brownlee GR, Nilsson SK, et al. The over-expression of HAS2, Hyal-2 and CD44 is implicated in the invasiveness of breast cancer. *Exp Cell Res* 2005;310:205–17.
15. Jung JE, Lee HG, Cho IH, et al. STAT3 is a potential modulator of HIF-1-mediated VEGF expression in human renal carcinoma cells. *FASEB J* 2005;19:1296–8.
16. Schmitt M, Horbach A, Kubitz R, et al. Disruption of hepatocellular tight junctions by vascular endothelial growth factor (VEGF): a novel mechanism for tumor invasion. *J Hepatol* 2004;41:274–83.
17. Nagano H. Treatment of advanced hepatocellular carcinoma: intraarterial infusion chemotherapy combined with interferon. *Oncology* 2010;78(Suppl 1):142–7.
18. Diaz BV, Lenoir MC, Ladoux A, et al. Regulation of vascular endothelial growth factor expression in human keratinocytes by retinoids. *J Biol Chem* 2000;275:642–50.
19. Hosui A, Hennighausen L. Genomic dissection of the cytokine-controlled STAT5 signaling network in liver. *Physiol Genomics* 2008;34:135–43.
20. Hosui A, Kimura A, Yamaji D, et al. Loss of STAT5 causes liver fibrosis and cancer development through increased TGF-{beta} and STAT3 activation. *J Exp Med* 2009;206:819–31.
21. Cui Y, Hosui A, Sun R, et al. Loss of signal transducer and activator of transcription 5 leads to hepatosteatosis and impaired liver regeneration. *Hepatology* 2007;46:504–13.
22. Onitsuka A, Yamada N, Yasuda H, et al. Rapid growth of hepatocellular carcinoma after or during interferon treatment of chronic hepatitis C: report of three cases. *Surg Today* 1996;26:126–30.

IJC
International Journal of Cancer

Inhibition of autophagy potentiates the antitumor effect of the multikinase inhibitor sorafenib in hepatocellular carcinoma

Satoshi Shimizu[1]*, Tetsuo Takehara[1]*, Hayato Hikita[1], Takahiro Kodama[1], Hinako Tsunematsu[1], Takuya Miyagi[1], Atsushi Hosui[1], Hisashi Ishida[1], Tomohide Tatsumi[1], Tatsuya Kanto[1], Naoki Hiramatsu[1], Naonobu Fujita[2], Tamotsu Yoshimori[2] and Norio Hayashi[3]

[1] Department of Gastroenterology and Hepatology, Osaka University Graduate School of Medicine, Suita, Osaka, Japan
[2] Department of Genetics, Osaka University Graduate School of Medicine, Suita, Osaka, Japan
[3] Kansai-Rosai Hospital, Amagasaki, Hyogo, Japan

Multikinase inhibitor sorafenib inhibits proliferation and angiogenesis of tumors by suppressing the Raf/MEK/ERK signaling pathway and VEGF receptor tyrosine kinase. It significantly prolongs median survival of patients with advanced hepatocellular carcinoma (HCC) but the response is disease-stabilizing and cytostatic rather than one of tumor regression. To examine the mechanisms underlying the relative resistance in HCC, we investigated the role of autophagy, an evolutionarily conserved self-digestion pathway, in hepatoma cells *in vitro* and *in vivo*. Sorafenib treatment led to accumulation of autophagosomes as evidenced by conversion from LC3-I to LC3-II observed by immunoblot in Huh7, HLF and PLC/PRF/5 cells. This induction was due to activation of autophagic flux, as there was further increase in LC3-II expression upon treatment with lysosomal inhibitors, clear decline of the autophagy substrate p62, and an mRFP-GFP-LC3 fluorescence change in sorafenib-treated hepatoma cells. Sorafenib inhibited the mammalian target of rapamycin complex 1 and its inhibition led to accumulation of LC3-II. Pharmacological inhibition of autophagic flux by chloroquine increased apoptosis and decreased cell viability in hepatoma cells. siRNA-mediated knockdown of the ATG7 gene also sensitized hepatoma cells to sorafenib. Finally, sorafenib induced autophagy in Huh7 xenograft tumors in nude mice and coadministration with chloroquine significantly suppressed tumor growth compared with sorafenib alone. In conclusion, sorafenib administration induced autophagosome formation and enhanced autophagic activity, which conferred a survival advantage to hepatoma cells. Concomitant inhibition of autophagy may be an attractive strategy for unlocking the antitumor potential of sorafenib in HCC.

Sorafenib is an orally available multikinase inhibitor recently approved as the first molecular targeting compound for hepatocellular carcinoma (HCC).[1] Sorafenib inhibits Raf kinases, including Raf-1 and B-Raf, which are members of the Raf/MEK/ERK signaling pathway, and inhibits a number of receptor tyrosine kinases involved in neo-angiogenesis and tumor progression, such as vascular endothelial growth factor receptor (VEGFR) 2, platelet-derived growth factor receptor β and c-Kit. Two randomized, placebo-controlled trials revealed that sorafenib significantly prolongs the median survival of patients with advanced HCC but the response is disease-stabilizing and cytostatic rather than one of tumor regression.[2,3] Therefore, a more detailed understanding of the mechanisms underlying both the antitumor effect and the primary resistance to this compound may provide insights that can help to improve the therapeutic outcome in HCC.

Macroautophagy (hereafter referred to as autophagy) is an evolutionally conserved catabolic process that transports cellular macromolecules and organelles to a lysosomal degradation pathway.[4] It is regulated by autophagy-related (*atg*) genes that control the formation and maturation of a double-membrane vesicle, autophagosome, which sequestrates cellular proteins and organelles. Autophagosomes then fuse with lysosomes to form autolysosomes, in which lysosomal enzymes digest the sequestered content and inner membrane. Autophagy is typically induced under starvation, initially considered to be a survival strategy that recycles cellular components to meet energy requirements. Autophagy also occurs at low basal levels in virtually all cells to perform homeostatic functions such as turnover of long-lived or damaged proteins and organelles. On the other hand, autophagy can mediate cell death under certain conditions probably through overactivation of self-digestion, which is considered to be Type II programmed cell death.[5] Therefore, autophagy can promote both cell survival and death depending on the cellular context and/or initiating stimulus.

Key words: liver, HCC, mTOR, tumor, apoptosis
Grant sponsors: Ministry of Education, Culture, Sports, Science and Technology, Japan; Ministry of Health, Labor and Welfare of Japan
*S.S. and T.T. contributed equally to this work and share first authorship.
DOI: 10.1002/ijc.26374
History: Received 4 Mar 2011; Accepted 3 Aug 2011; Online 19 Aug 2011
Correspondence to: Tetsuo Takehara, Department of Gastroenterology and Hepatology, Osaka University Graduate School of Medicine, 2-2 Yamada-oka, Suita, Osaka 565-0871, Japan, Tel.: +81-6-6879-3621, Fax: +81-6-6879-3629, E-mail: takehara@gh.med.osaka-u.ac.jp

Autophagy has been shown to be involved in cancer development and progression in a variety of ways.[6] Genetic evidence supports a tumor suppressive role of autophagy in cancer development. The *Beclin 1* autophagy gene is monoallelically deleted in a subset of human sporadic breast, ovarian and prostate cancer. Heterozygous disruption of *Beclin 1* increases the frequency of spontaneous malignancies in mice.[7] On the other hand, tumor cells display autophagy or autophagic cell death under a variety of stress-inducing conditions as well as anticancer therapies.[8] Therefore, autophagy promotes or inhibits tumor progression which is also dependent on the cell types and stimuli. Recently, sorafenib has been reported to induce autophagosome accumulation, as evidenced by GFP-LC3 markers, in tumor cells.[9–11] However, its biological and clinical significance has not yet been addressed. In the present study, we examined autophagy of hepatoma cells treated with sorafenib and demonstrate that sorafenib not only induces autophagosome formation but also activates autophagic flux which is an adaptive response to this compound, and that concomitant inhibition of autophagy may be therapeutically useful for improving the anti-HCC effect.

Material and Methods

Cell lines

Hepatoma cell lines Huh7, HLF and PLC/PRF/5 were cultured with Dulbecco's modified Eagle medium (DMEM). Huh7 and HLF were obtained from the JCRB/HSRRB cell bank (Osaka, Japan) and PLC/PRF/5 was obtained from ATCC (Manassas, VA). All cell lines were cultured at 37°C in a humidified atmosphere of 5% CO_2.

Western immunoblot

Cells or tissues were lysed and immunoblotted as previously described.[12] For immunodetection, the following antibodies were used: anti-microtubule-associated protein 1 light chain (LC3) polyclonal antibody (Ab) (MBL, Nagoya, Japan); anti-ATG7 polyclonal Ab (MBL); anti-Beclin1 polyclonal Ab (CST, Danvers, MA); anti-p62 polyclonal Ab (MBL); anti-phospho-ERK polyclonal Ab (CST); anti-phospho-S6K polyclonal Ab (CST); anti-phospho-4E-BP1 polyclonal Ab (CST); anti-phospho-Akt polyclonal Ab (CST).

Transfection with fluorescent LC3 plasmid

Cells were transfected with monomeric red fluorescence protein (mRFP)-GFP tandem fluorescent-tagged LC3 expression plasmid (ptfLC3)[13] using Fugene6 (Roche Applied Science, Hague Road, IN) according to the manufacturer's instructions. At 48 hr after transfection, the medium was changed to DMEM containing sorafenib or DMSO, and the cells were further cultured and examined under a BZ8100 fluorescent microscope (Keyence, Osaka, Japan).

In vitro treatment with sorafenib

Hepatoma cells were transfected with 5 nM Silencer Select siRNAs (Ambion, Austin, TX) either of *ATG7* or negative control using RNAiMAX (Invitrogen, Carlsbad, CA) according to the manufacturer's instructions. Forty-eight hours after transfection, the medium was changed to DMEM containing sorafenib or DMSO. Cells were further cultured and assayed for cell viability by WST assay using the cell count reagent SF (Nacalai Tesque, Kyoto, Japan) and analyzed for apoptosis using Annexin V-FITC apoptosis detection kit (Biovision, Mountain View, CA). We defined apoptotic cells as Annexin V-FITC positive and propidium iodide (PI) negative cells. PI negative cells were gated and the positive cell rate of Annexin V-FITC was determined. The supernatant of the cultured cells was assayed for caspase-3/7 activity using Caspase-Glo 3/7 assay (Promega, Madison, WI) as previously reported.[12] For the treatment with a pharmacological inhibitor of autophagy, cells were cultured with DMEM containing chloroquine (Sigma-Aldrich, St. Louis, MO) or bafilomycin A1 (Sigma-Aldrich) with sorafenib or DMSO and assayed for cell viability and caspase-3/7 activity in the same manner.

Electron microscopy

Samples were fixed with 2.5% glutaraldehyde solution buffered at pH 7.4 with 0.1 M Millonig's phosphate at 4°C for 2 hr, postfixed in 1% osmium tetroxide solution at 4°C for 1 hr, dehydrated in graded concentrations of ethanol and embedded in Nissin EM Quetol 812 epoxy resin. Ultrathin sections (80 nm) cut on a Reichert ultramicrotome (Ultracut E) were stained with uranyl acetate and lead citrate, and examined with a Hitachi H-7650 electron microscope at 80 kV.

Xenograft experiments

To produce a xenograft tumor, 3–5 $\times$ 10^6 Huh7 cells were subcutaneously injected to Balb/c nude mice. Sorafenib tablets were crushed and orally administered daily with water containing 12.5% cremophor EL (Sigma-Aldrich) and 12.5% ethanol, as previously described.[14] Chloroquine was dissolved in PBS and intraperitoneally administered daily. We estimated the volume of the xenograft tumor using the following formula: tumor volume = $\pi/6 \times$ (major axis) $\times$ (minor axis)^2. Mice were maintained in a specific pathogen-free facility and treated with humane care with approval from the Animal Care and Use Committee of Osaka University Medical School.

Statistical analysis

Data are presented as mean $\pm$ SD. Comparisons between two groups were performed by unpaired t test. Multiple comparisons were performed by ANOVA with Scheffe post-hoc test. $p < 0.05$ was considered statistically significant.

Results

In vitro treatment with sorafenib induces accumulation of autophagosomes in hepatoma cell lines

To examine the effect of sorafenib on autophagy in human HCC, we treated the hepatoma cell line Huh7 with sorafenib *in vitro*. First, we assessed the expression of LC3, a

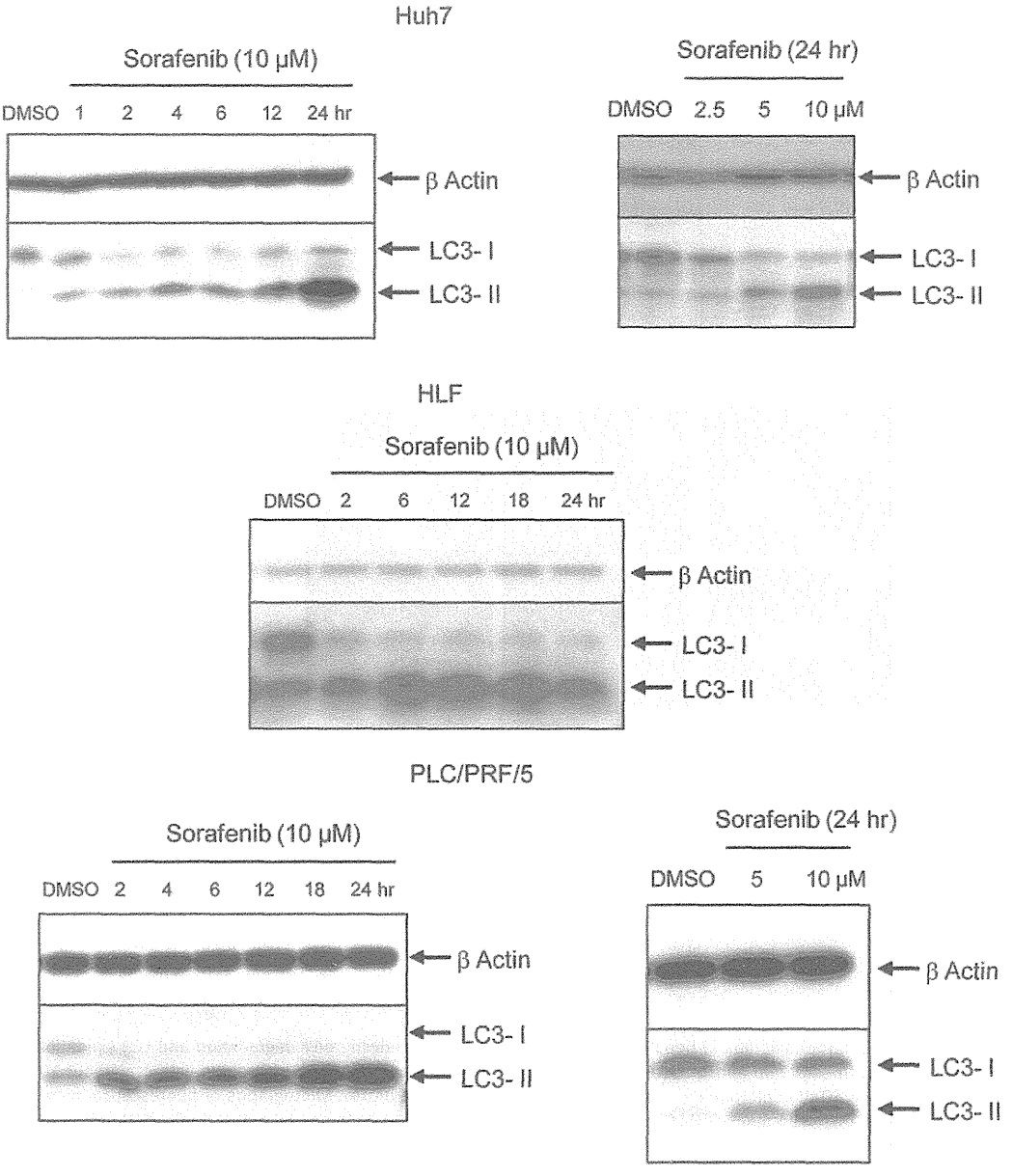

Figure 1. Sorafenib induces accumulation of autophagosomes in hepatoma cells. Western blot showing an increase in LC3-II in Huh7, HLF and PLC/PRF/5 hepatoma cells after treatment with sorafenib. Hepatoma cells were treated with 2.5, 5 or 10 μM sorafenib for the indicated times and analyzed for LC3 expression by western blot. Hepatoma cells treated with DMSO-containing media for 24 hr are shown as the control. [Color figure can be viewed in the online issue, which is available at wileyonlinelibrary.com.]

mammalian homolog of yeast *atg8*, by immunoblot. During the progress of autophagy, the cytoplasmic form LC3-I is converted to the membrane-bound lipidated form LC3-II which is detected by a mobility shift on electrophoresis.[15] When Huh7 cells were treated with 10 μM sorafenib, LC3 conversion was observed as early as 1 hr after the treatment and gradually increased at later time points (Fig. 1). We examined the dose-dependency of this response in Huh7 cells as well. Under 2.5 μM sorafenib treatment, the amount of LC3-II did not show an obvious increase, however, the amount of LC3-I decreased which indicates modest activation of autophagosome formation. Under 5 and 10 μM sorafenib treatment, the amount of LC3-II clearly increased. Next, we investigated the effect of sorafenib on other hepatoma cell lines, HLF and PLC/PRF/5. Under sorafenib treatment, LC3 conversion was observed at 2 hr after the initiation of treatment and gradually increased until 24 hr in HLF cells and PLC/PRF/5 cells in the same manner as in Huh7 cells.